IEEE Access
Multidisciplinary ⋮ Rapid Review ⋮ Open Access Journal

Received March 23, 2022, accepted April 10, 2022, date of publication April 18, 2022, date of current version April 28, 2022.

Digital Object Identifier 10.1109/ACCESS.2022.3168727

A Comprehensive Analysis of Wireless Charging Systems for Electric Vehicles

NAOUI MOHAMED [1], FLAH AYMEN [1], TURKI E. A. ALHARBI [2], CLAUDE ZIAD EL-BAYEH [3], SBITA LASSAAD [1], SHERIF S. M. GHONEIM [2], (Senior Member, IEEE), AND URSULA EICKER [4]

[1]Research Unit of Energy Processes Environment and Electrical Systems, National Engineering School of Gabes, University of Gabés, Gabés 6029, Tunisia
[2]Department of Electrical Engineering, College of Engineering, Taif University, Taif 21944, Saudi Arabia
[3]Department of Electrical Engineering, Bayeh Institute, Amchit 110393, Lebanon
[4]Canada Excellence Research Chair Team, Concordia University, Montreal, QC H3G 1M8, Canada

Corresponding author: Naoui Mohamed (mednaouiing@yahoo.com)

This work was supported in part by the Canada Excellence Research Chair in Smart, Sustainable and Resilient Communities and Cities; in part by the Natural Sciences and Engineering Research Council of Canada (NSERC) Discovery under Grant RGPIN-2016-06727; and in part by the Taif University Researchers Supporting, Taif University, Taif, Saudi Arabia, under Project TURSP-2020/34.

ABSTRACT In the coming years, major transportation sectors will be electrified, in which more accessible and easy solutions for charging Electric Vehicles (EVs) become vital. Wireless charging is considered one of the best and easiest methods to charge EVs anywhere, even during the driving of cars. To get accurate charging power rates while charging wirelessly, advanced mathematical models are needed to accurately present the charging power. Such models must take into consideration all the coils parameters, shapes, the used compensation topology, and if the system is static or dynamic. This paper presents a comprehensive analysis of the wireless charging systems adapted for EVs by stating the most common charging topologies, and architectures, and by concentrating on the corresponding mathematical models used to calculate the given electrical power as a function of the EV's situation on streets and its speed. Then, it is possible to evaluate the EV autonomy, and an accurate approximation can be determined when EV is on a wireless charging road. Even with the citation and comparison between the two studied models, this paper opens some perspectives for energy transmitter tools and tries to explain how renewable energy can help the deployment of this technology.

INDEX TERMS Dynamic mode, electric vehicle, modeling, static mode, topologies, wireless recharge, renewable energy.

ABBREVIATIONS

EVs	Electric Vehicles.
HEV	Hybrid Electric Vehicles.
WPT	Wireless Power Transfer.
IPT	Inductive Power Transfer.
V2G	Vehicle to Grid.
WCSEV	Wireless Charging System for Electric Vehicle.
W-V2G	Wireless Vehicle to Grid.
S-WCSEV	Static Wireless Charging System for EV.
D-WCSEV	Dynamic Wireless Charging System for EV.
DS-WCSEV	Dynamic and Static Wireless Charging System for EV.

LIST OF SYMBOLS

M	Mutual inductance (H).
Ω	Oscillation angular frequency (rad/sec).
k	Magnetic coupling constant.
L_s	Secondary inductance (H).
L_p	Primary inductance (H).
Z_p	Primary impedance (Ω).
Z_s	Secondary impedance (Ω).
I_p	Primary current (A).
I_s	Secondary current (A).
V_p	Primary voltage (V).
V_s	Second voltage (V).
I_1	Source current (A).
I_2	Load current (A).
C_s	Secondary capacitance (F).
C_p	Primary capacitance (F).
Q_1	Primary and secondary quality factors.
Q_2	secondary quality factors.
P_s	Secondary power (W).
P_p	Primary Power (W).
L_a	Primary leakage inductance (H).
L_b	Secondary leakage inductance (H).

The associate editor coordinating the review of this manuscript and approving it for publication was Asad Waqar Malik.

R_L Load (Ω).
η The efficiency of the power transfer (%).
η_2 Efficiency of the second part.
η_1 Efficiency of the primer part.
Z_1 The global impedance of the primary coil (Ω).
V_1 Source voltage (V).
R_s Secondary resistance (Ω).
R_p Primary resistance (Ω).
n_c Number of receiver coils.
$r1$ Primary radius (m).
$r2$ Secondary radius (m).
h Height (m).
μ_0 Permeability of free space (H/m).

I. INTRODUCTION

The number of electric vehicles (EVs) has been steadily growing since the beginning of the 21st century [1]. However, the limitations of the charging time of the battery [2] and the autonomy are a hindrance to the use of the technology [3]. The direct consequence is the intrusion of chargers and power cables into our daily lives, which increasingly tends to limit the mobility offered by vehicles [4]–[6]. Much research effort has gone into solving these problems, and wireless power transfer (WPT) to EVs has become evident and feasible to solve this problem [7]–[9]. Many years ago, WPT systems using high intensity, time-varying electromagnetic fields were presented. But at that time, there was little need for the WPT, because cable power distribution systems were generally more efficient and less expensive for electrical devices. Today, wireless short-range power transfer devices using electromagnetic induction are used more and more in industrial products for contactless charging [10]. However, due to the limitation of the transfer distance of the energy, this technology cannot charge EVs to cover distances of more than one-fifth (1/5) the dimension of the power transmitter [11]. An improved method based on resonant coupling showed efficient results for extending the transfer distance to more than 2 or 3 times the size of the transmitter or receiver [12].

A few years later, the Wireless power transfer transmission for EVs evolved, which can overcome the disadvantages of wired chargers and remove specific barriers to vehicle electrification and long-term mobility [13]. Aside from being more convenient than wired chargers, WPT allows for substantial reductions in the size of the onboard EV battery [14]. Also, electric buses were considering the stationary WPT charging method. The onboard battery can be reduced by at least two-thirds [15] due to passengers' regular loading and unloading at bus stations. Because of these in-route costs, it is possible to hold a much smaller onboard battery and still meet the vehicle route specifications [1]. Adding to the Wireless Power Transfer technology, the Inductive Power Transfer (IPT) techniques are widely available in the market, while resonance IPT techniques are emerging in the consumer market [16]. Furthermore, the car industry plans to use IPT for all-electric vehicles to facilitate the charging process and improve drivers' satisfaction.

Despite the significant development of the charging solution, this system still contains many defects and problems that have been developed and are still scalable. Major related drawbacks were treated in [17]. In this work, the authors analyzed the discrepancies in the loop design of the coils and the electromagnetic shielding elements for wireless charging systems and showed the negative effect of electromagnetic interference on the system's efficiency. Also, in [8], the authors presented the problem of coils position, the impact of the number of receiver coils, and the influence of the distance between the transmitter and receiver. The authors pointed out that these elements have negative impacts on the quality of given electrical power. Also, they explained that the coil parameters concerning the used metal type, have significant impacts on efficiency. On the other side, it is essential to mention that the automotive interior will be influenced by the high frequency resonant provided by the transmitter. Especially, if the wireless charging tool is used, when the EV is charging. Many research papers are developing new technologies and methods to improve the conditions for using wireless charge systems.

In [18] and [19], the authors investigated dynamic and static modeling to improve the efficiency of the EV wireless charging systems. The inspected model relied on the mutual inductance related to primary and secondary coils. It was studied only for the case of superimposing the receiver and transmitter coils. They also referred to the thermal concerns of automotive interior and the problem of preventing thermal failure within high-power ferrite structures of EV wireless charging inductive power transfer.

All these wireless power transfer technologies and solutions must be summarized, discussed, and explained to understand their architectures and topologies. Furthermore, by knowing the efficiency of each topology, it is important to determine the mathematical model and its parameters that can be used for each application.

One of the main objectives of our work in this paper is to discuss the WPT systems, give the possible used topologies, and recommend possible shapes that can be applied. On the other hand, our analysis shows a detailed mathematical investigation of the WPT functionally, considering all the possible operation modes, whether static or dynamic. The present work defines all the possible variables and parameters that can be used to build a solid mathematical model in both static and dynamic situations. The proposed mathematical model can be firstly used to calculate the quantity of power transferred from the transmitter to the receiver. Then, we expose and explain the needed equations for dimensioning and sizing the coil transmitters or receivers. Hence, the obtained model estimates the potential stored energy and guesses the EV's autonomy.

The remainder of the paper is presented as follows. Section 2 is related to the wireless charging system and the different types of WPT for EVs. In Section 3, we discuss

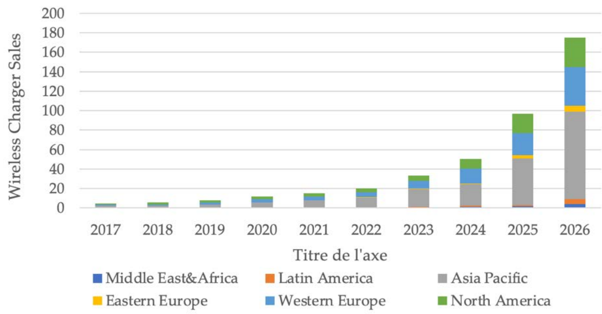

FIGURE 1. Classification of the wireless charger number by region for 2017-2026 [2].

the evolution of static and dynamic models for the most commonly used WPT. In Section 4, a comparison of different models in scientific research is shown. Section 5 discusses the future applications and concepts of wireless charging systems for EVs (WCSEV). Finally, Section 6 illustrates the conclusion and outlines some future trends.

II. WIRELESS CHARGING SYSTEMS FOR EVs

The EV charging systems and techniques were primarily developed to solve the problems of low autonomy of the car and increase the range anxiety to cover the road distance for a specific trip. Major EV manufacturers have developed various solutions to help charge EVs during their trips, such as installing charging stations, charging points, and even wireless charging pads buried under the highways. Also, several attempts to eliminate the connected charger solutions require the EVs to stop for several minutes or hours and charge using physical connection cables. Therefore, it becomes necessary to shift to wireless charging solutions to increase the satisfaction of the EV owners and reduce their stress while waiting for their cars to charge. Hence, some of the presented solutions in this paper are based on the wireless charging methods to reduce all the previously cited weaknesses of using physical charging cables. Wireless charging is a viable option when drivers cannot be counted on to charge their EVs regularly, such as in shared vehicle systems or fleets [20]. This wireless charging method was firstly used in homes, and then it became a public solution placed in many parking zones. Fig.1 presents the projected wireless charger system, sales by region, for 2017 to 2026 [2].

A. THE WIRELESS CHARGING SYSTEM DESCRIPTION

Using induction charging technology, electric car manufacturers intend to make it easier for future owners of these vehicles to charge their batteries. The system is based on a first plate placed on the ground that incorporates a primary coil that will emit an alternating magnetic field to a second plate with a secondary coil installed under the electric or plug-in hybrid vehicle. This system works when the car is parked over the primary coil, and the two plates are perfectly aligned; wireless charging allows a battery to be refilled safely under

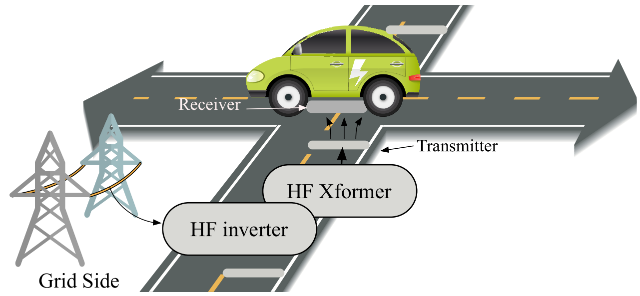

FIGURE 2. Dynamic wireless power transfer for a receiver coil for each car.

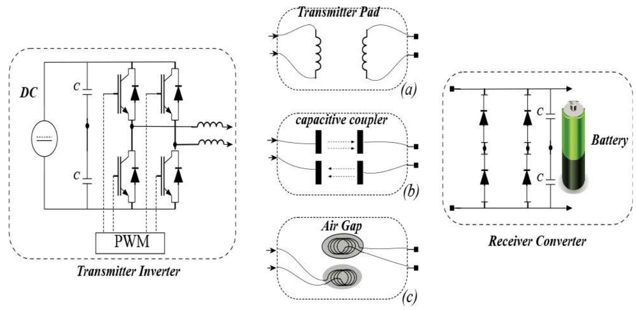

FIGURE 3. (a) Inductive power transfer (b) Capacitive wireless power transfer, (c) Magnetic wireless power transfer.

all weather conditions. This type of charging achieves 80% to 90% efficiency compared to traditional charging cable tools. Charging, therefore, takes longer than if the car was plugged in. For example, fully charging a battery pack should take around one-hour using cables and 1.11 hours using wireless charging (at an efficiency of 90%) [21], [22]. A simple block diagram for the wireless charging systems (WCs) is shown in Fig. 2. On the grid side, a high-frequency inverter (HF inverter) is connected to the Xformer inverter. Then, the power is delivered to the transmitter [23].

Three main methods for developing wireless charging systems for electric vehicles (WCSEV) have been used since the advent of wireless charging: (a) inductive power transfer (IPT), (b) conventional capacitive wireless power transfer (CWPT), and (c) magnetic gear wireless power transfer (MGWPT). Some review papers on the wireless power transfer (WPT) technologies for battery-operated electric vehicles (BEVs) can be found in references [24]–[28]. Fig. 3 presents the three major wireless charging methods.

1) INDUCTIVE POWER TRANSFER

The traditional inductive power transfer was created in 1914 by Nikola Tesla to transmit electricity wirelessly. Magnetic induction WPT is a well-known technique that has long been used in transformers, in which a primary coil and a secondary coil are inductively coupled [29]. For example, through the use of a common permeable magnetic core. The energy transmission by induction in air, in which the primary coil and the secondary coil are physically separated, has also been a technique known for over a century. The close-coupled

WPT technique's power transmission efficiency decreases when the distance in the air is superior to the diameter of the coil, and the coils are not aligned within the distance. The efficiency of energy transmission is determined by the coupling factor and the quality of the inductors. This technique outperforms the magnetic resonance method in terms of efficiency. This technology is available in the market, such as charging smartphones wirelessly. With an array of coils, the close-coupled WPT technique also offers some flexibility regarding the location of the receiver coil relative to the transmitter [30].

2) CAPACITIVE WIRELESS POWER TRANSFER

The capacitive coupling of the WPT system has two circles of electrodes and does not use coils as in the case of magnetic-type WPT systems [31], [32]. Energy is diffused through an induction field produced by the coupling of the two sets of electrodes. The capacitive coupling system has the following advantages: (i) The capacitive coupling system offers flexibility for horizontal positioning with an easy-to-use charging system for end-users, (ii) a very thin electrode (less than 0.2 mm) can be used between the transmitter and receiver of the system, (iii) no heat generation in the wireless power transmission area. The temperature does not rise in this area, so the battery is protected against heat even when placed nearby [33]. The emission level of the electric field is low due to the structure of the coupling system. The electric field emanates from the electrodes and provides the transmission of energy. The low-cost structures and simplicity of capacitive wireless power transfer (CWPT) technology benefit low-power applications, such as pacemakers, neurostimulators, cochlear implants, etc., [31]–[33]. In the CWPT, instead of using coils or magnets, coupling capacitors pass power from the source to the receiver. Via power factor correction circuitry, the principal AC voltage is applied to an H-bridge converter [32], [34], [35].

3) MAGNETIC WIRELESS POWER TRANSFER

The magnetic gear wireless power transfer (MGWPT) differs from the capacitive and inductive power transfers [29]. Magnetic resonance WPT is also referred to as weak coupling WPT. The theoretical principle of this magnetic resonance method was developed in 2005 by the Massachusetts Institute of Technology, and it was validated experimentally in 2007. The method uses a coil and a capacitor as a resonator, in which electrical energy is transmitted through electromagnetic resonance between the transmitter and the receiver coils [36]. By matching the resonant frequency of the two coils with a high factor, significant amounts of electrical energy can be transmitted. The magnetic coupling between the transmitter and the receiver coils is weak. This technique also provides flexibility in the location of the receiver coil relative to the transmitter coil. Applied technical details can be found in many technical publications, such as in [37].

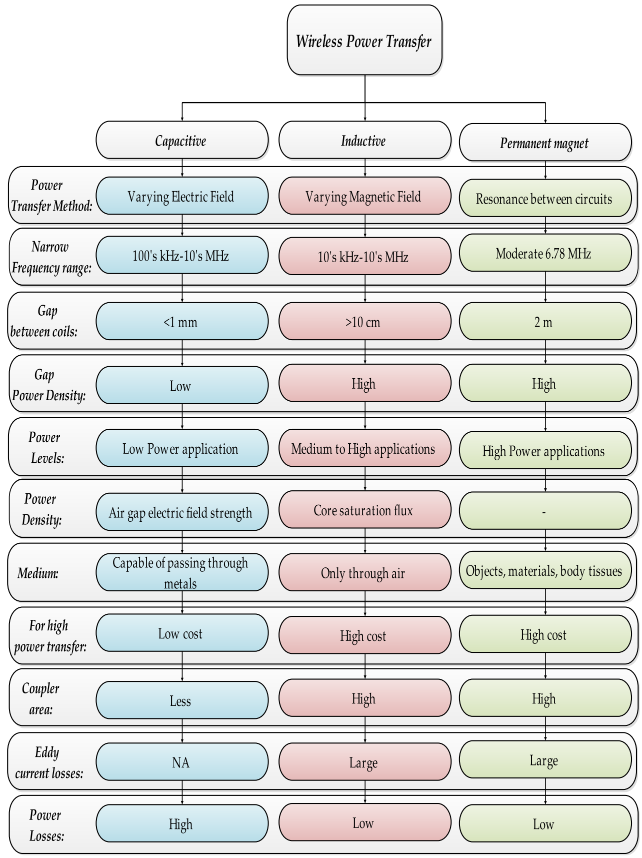

FIGURE 4. Latest architectures of wireless power transfer in 2020.

TABLE 1. Comparison of different WPT architectures for EV applications.

WPT	Suitability for WCSEV	Power Level	Complexity of design	Size/ Volume
Capacitive	Low/Medium	Low	Medium	Low
Inductive	High	Medium/High	Medium	Medium
Permanent magnet	Low/Medium	Medium/Low	High	High

TABLE 2. Performance of WPT in EVs.

WPT	Coupling efficiency	EMI*	Frequency range (kHz)	Power Transferred	Distance
Capacitive	Medium	Medium	100–600	3.7 W	0.13 mm
Inductive	High	Medium	10–50	100 kW	127 mm
Permanent magnet	Medium	High	0.05–0.500	818 kW	50 mm

**Electromagnetic interference (EMI)*

4) COMPARING DIFFERENT NEAR-FIELD TRANSMISSION TECHNIQUES

The development of wireless charging systems has been accelerating since 2009. Each system has some advantages and disadvantages, and the characteristics of each system of the near-field transmission techniques are compared in Tables 1 and 2, and Fig. 4 [38]–[43].

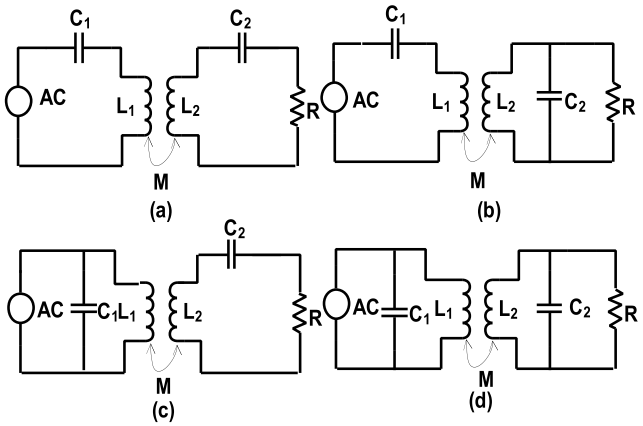

FIGURE 5. WPT topologies: (a) SS, (b) SP, (c) PS, and (d) PP.

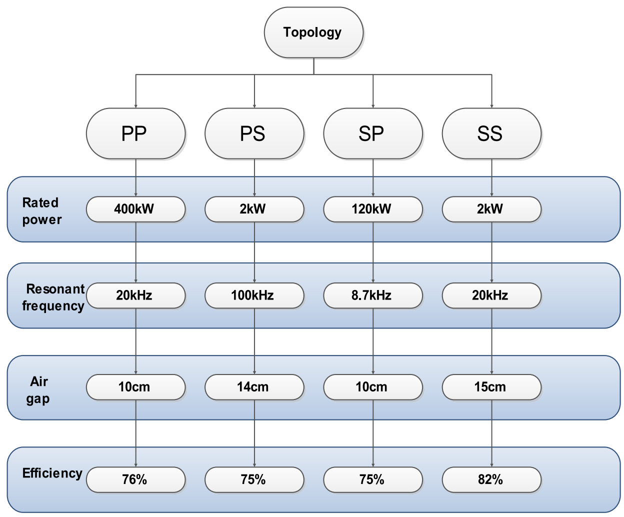

FIGURE 6. Features of compensation topologies.

TABLE 3. Parameters of compensation topologies.

Features	(SS)	(SP)	(PS)	(PP)
Primary capacitor	$\frac{1}{\omega^2 L_P}$	$\frac{1}{\omega^2\left(L_P-\frac{M^2}{L_s}\right)}$	$\frac{1}{\omega^2\left(L_P-\frac{\omega^2 \cdot M^4}{L_P \cdot R_{load}}\right)}$	$\frac{1}{\omega^2\left(\left(L_P-\frac{M^2}{L_s}\right)+\frac{\frac{M^4}{L_s^4}\cdot R_{load}^2}{\omega^2\cdot\left(L_P-\frac{M^2}{L_s}\right)}\right)}$
Secondary capacitor	$\frac{1}{\omega^2 L_s}$	$\frac{1}{\omega^2 L_s}$	$\frac{1}{\omega^2 L_s}$	$\frac{1}{\omega^2 L_s}$
Load	$\frac{\omega L_s}{Q_s}$	$\omega L_s Q_s$	$\frac{\omega L_s}{Q_s}$	$\omega L_s Q_s$

SS: series-series, SP: series-parallel, PS: parallel-series, PP: parallel-parallel.

TABLE 4. A brief comparison of various coil shapes [44].

Type of Coil	Criteria for comparison		
	Polarization type	Path of Flux	The Null Zone
Circular	Non-Polarized perpendicular flux generation	one-quarter of the pad's diameter	40%
Rectangular coil	Non-Polarized perpendicular flux generation	Almost the same as the pad diameter	50%
Double-D	Generation of polarized, parallel fluxes	The circular motion is repeated twice.	77%
Quad-D quadrature	Small sections are polarized, and perpendicular flux reigns supreme.	4/5 of the length of the pad	This is not the case for the extended transmitter.

B. COMPENSATION TOPOLOGIES & COILS PARAMETERS

In the WPT systems, four resonant circuit topologies can be used [44]. After inserting the capacitor on each side, their indexation is completed. Therefore, the topologies can be described as follows: Series-Series (SS), Series-Parallel (SP), Parallel-Series (PS), and Parallel-Parallel (PP). These designs can be shown in Fig. 5 [45], [46]. The inductances and capacitors (C_1, C_2) are determined to cancel the reactive part of the transferred power. The primary and secondary circuits (L, C) of the coupler are used to enhance the transfers and minimize the apparent power of the input source while ensuring active power transmission to the load [47], [48]. The principal disadvantages are the high values of voltage or current related to the resonance components. The additional benefits and features of various compensation networks used in the inductive power transfer for EVs are shown in Table 3, and each topology feature can be shown in Fig. 6 [21], [49], [50].

C. COIL DESIGN FOR CHARGING SYSTEMS

In wireless power transfer, an air-core wireless transformer proposal is used to transfer electrical power from the source to the receiver sides. Fig. 7 depicts the various designs for the WPT system; numerous planar coil shapes, including circular, rectangular, and hybrid configurations, were used to recover performance and solve misalignment issues among the transmitter and receiver [51]. Table 4 lists the specifications for each model [44], as well as the advantages and disadvantages of each model [52]. Multiple wireless power transfer structures for motorized applications are evaluated in the literature to assess magnetic couplings and feasibility. Most of these studies focused on structures with circular designs, and recently [53] and [54] tested a circular planar structure for a 2 kW inductive power transfer. It has been demonstrated that the null zone is the least one that faces the other models. The performance of resonant coupling power transmission is primarily determined by the performance of the used resonators. A good resonator for WPT should have a high Q factor and a high coupling coefficient, which is the ratio of mutual inductance to self-inductance [55]. The comparison of different types of resonators is listed in Table 5, [56].

III. EVOLUTION OF WPT STATIC & DYNAMIC MODELS

The manipulation of the energy from wireless charging models must be studied according to the load position and specifications. Generally speaking, there are two types. The first one is linked to a static position, and the second one is linked to a dynamic position [57]. Here, the nomination of static or dynamic is related to the receiver's position facing the transmitter, (i.e., if it is in stationary or displacement modes). To study properly the charging system, it is essential to

TABLE 5. Comparisons of different resonators.

Definition	Solenoid-type resonators	Spiral (or ring) resonators	Ceramic dielectric resonators
Frequency range	~1MHz to ~100MHz	~1MHz to ~100MHz	~0.5GHz to ~10GHz
Mechanisms of loss	Conduction losses, Radiation losses	Conduction losses, Radiation losses	Conduction losses, Dielectric losses
Coupling coefficient	High	High	Average
Transfer distance	0,05m to 5m	0,05m to 5m	0,01m to 0,2m
Cost	Small	Small	Average

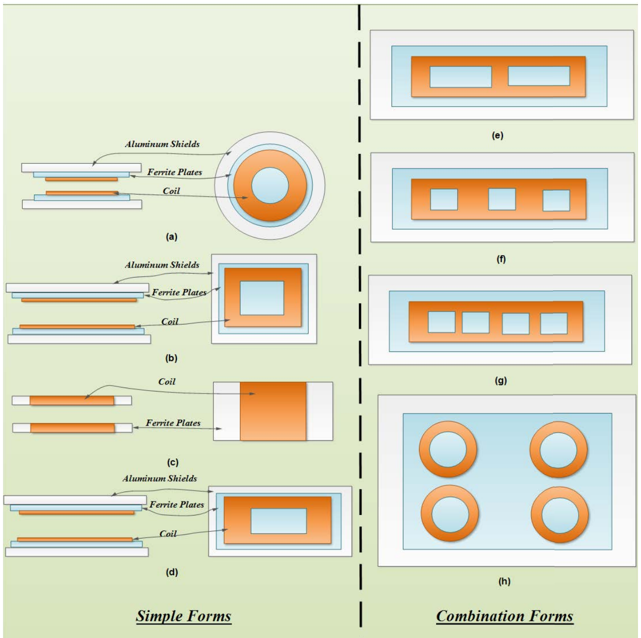

FIGURE 7. Different coil shapes for the receivers and transmitters.

define the corresponding mathematical equations and model for each case and present the relationship between different parameters and variables that can affect the functionality of this system [58].

A. STATIC WIRELESS CHARGING SYSTEM FOR EV (S-WCSEV)

The S-WCSEV defines the case where the receiver coil placed under the vehicle is aligned with the transmitter coil placed on the road, as in Fig. 8. This applies to stationary EVs. Then, it is possible to define if the received power is maximum or minimum [50]. It depends on the position center of the two coils. In [59], the authors showed that when the distance between the centers' increased, the received power decreased [13]. If the receiver radius is more significant than the distance between the two middles, the transferred power is null. Fig. 8 shows the distance between the two coils. It is mentioned that two coils are aligned if D1 = 0, [5].

1) A PRIMARY MODELING FORM

A primary modeling form of the S-WCSEV was studied in [60], in which the authors considered static modeling to improve the WPT. Hence, a simplified model of this power

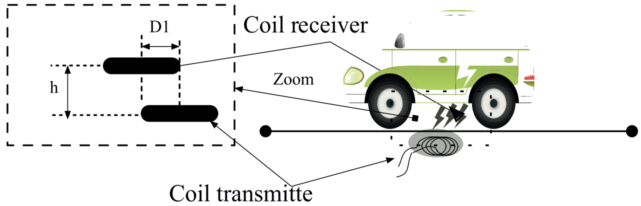

FIGURE 8. Distance between the center of the two coils in static mode.

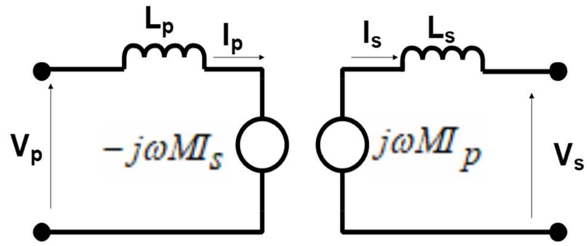

FIGURE 9. A simplification design for an IPT.

transfer system using IPT can be presented in Fig. 9. The input and output voltages of the IPT are denoted by V_P and V_S.

The induced and reflected voltages in this model are described in terms of mutual inductance M, angular frequency ω, and primary and secondary currents I_p and I_s. The magnetic coupling coefficient is related to mutual inductance, as in Eq. (1). The reflected impedance Z_r from secondary to primary can be calculated as in Eq. (2), [61]. Where, Z_s is the secondary system's impedance, which is determined by the compensation topology chosen.

$$k = \frac{M}{\sqrt{L_p L_s}} \tag{1}$$

$$Z_s = \frac{\omega^2 M^2}{Z_r} \tag{2}$$

The current passing through the secondary winding is defined in Eq. (3). As a result, the voltages across the primary and secondary windings are given by Eq. (4).

$$I_s = \frac{j\omega M I_p}{Z_s} \tag{3}$$

$$\begin{cases} V_p = j\omega L_p I_p - j\omega M I_s \\ V_s = j\omega M I_p - j\omega L_s I_s \end{cases} \tag{4}$$

The primary and secondary frequencies are the same as calculated in Eq. (5). The primary and secondary power levels are defined by Eq. (6).

$$\omega = \frac{1}{\sqrt{C_s L_s}} = \frac{1}{\sqrt{C_p L_p}} = 2\pi f \tag{5}$$

$$\begin{cases} P_p = V_p I_p \\ P_s = V_s I_s \end{cases} \tag{6}$$

With wireless charging systems to recover multiply all receivers (coil and capacitor) are typically designed identically, the total impedance reflected from all sensors (coil

TABLE 6. Parameters of the secondary impedance.

Parameter	Series	Parallel
Secondary impedance Z_s	$j\omega L_s + \frac{1}{j\omega C_s} + R$	$j\omega L_s + \frac{1}{j\omega C_s} + \frac{1}{R}$
Load current I_L	I_s	V_s/R
Load voltage V_L	$I_s R$	V_s
Reflected reactance	0	$-\frac{\omega_0 M}{L_s}$
Reflected resistance	$\frac{\omega_0{}^2 M^2}{R}$	$\frac{RM}{L_s{}^2}$
Secondary Quality factor Q_s	$\frac{\omega_0 L_s}{R}$	$\frac{R}{\omega_0 L_s}$

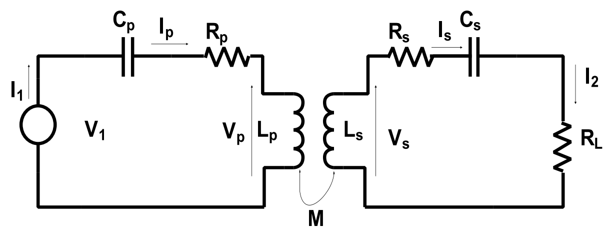

FIGURE 10. Design of SS topology with the load.

and capacitor) is defined by Eq. (7). The number of receiver coils is denoted by n. The equivalent coupling coefficient and mutual inductance are then determined by Eq. (8) and (9).

$$\sum_{i=1}^{n} Z_{ri} = n\frac{\omega^2 M^2}{Z_s} \tag{7}$$

$$\begin{cases} k_n = k\sqrt{n} \\ 0 \le k \le 1 \end{cases} \tag{8}$$

$$M_n = \mathrm{M}\sqrt{n} \tag{9}$$

Table 6 also shows the reproduced resistance and reactance estimated from Eq. (2) at the secondary resonant frequency, which depends on the utilized compensations.

2) A SECOND MODELING FORM

A second modeling method was presented in [62], [63], in which the authors studied the static case and looked for the parameters that can be optimized to boost the system. The model is based on the mutual inductance calculation step, considering the position, and primary and secondary coil parameters. Based on these studies, the SS architecture is the most commonly studied form with the corresponding topology shown in Fig. 10. Parameters are calculated considering variable characteristics, such as resistances, inductances, and mutual inductance.

It was stated that $L_a = L_p - M$ and $L_b = L_s - M$, respectively, present the primary and secondary winding leakage inductances. The primary voltage of the coil is denoted V_p in this model, and it is supplied by a sinusoidal voltage source denoted V_1. In this case, R_L denotes a serial resistive load that is used to generate the final expression of the global yield value, as in Eq. (15). Eq. (10) depicts the power consumption when a resistive load is attached, taking the mutual inductance parameter as a function of the primary current into account. Eq. (11) is used to express the global impedance of the primary coil. As a result, the equivalent primary current can be calculated as in Eq. (13).

$$P_{wr} = I_P^2 \left(\frac{(\omega M)^2}{R_L} \right) \tag{10}$$

$$Z_1 = \frac{(M\omega)^2}{j\omega (L_b + M) - \frac{j}{\omega C_s} + R_s + R_L} + j\omega (L_a + M) - \frac{j}{\omega C_p} + R_p \tag{11}$$

$$I_1 = V_1/Z_1 \tag{12}$$

where, C_p and C_s, are the primary and secondary capacitance dimensions that must be evaluated using a null imaginary part of Z_1. The equation can then be used to express the corresponding Eq. (13) of the related capacitance. Using Eq. (14), the energetic yield of the WPT system can be calculated. The resistance value has a significant impact on the yield because it is assumed to be a real load within the overall system. It is found that the system transmission strength is only affected by the reciprocal inductance between the primary and secondary side coils. The reduction of variable parameters simplifies the study of transmission power stability; hence, the system efficiency is given by Eq. (15). In Eq. (15), R_L is the secondary-side load impedance, whereas R_s and R_p represent the internal impedances of the secondary and main sides, respectively. The load and internal impedance are constant when the charging system is definite. As a result, it is possible to deduce that the system efficiency is solely determined by mutual inductance between the primary and secondary side coils.

$$C_p = C_S = \frac{1}{\omega^2 (L_b + M)} \tag{13}$$

$$\begin{cases} \eta = \dfrac{\left|\vec{I}_2\right| R_L}{\left|\vec{I}_P\right|^2 R_P + \left|\vec{I}_s\right|^2 R_s + \left|\vec{I}_s\right|^2 R_L} \\ \dfrac{|I_P|}{|I_2|} = \dfrac{R_S + R_L}{\omega M} \end{cases} \tag{14}$$

$$\eta = \frac{R_L}{R_L + R_S + \left(\frac{R_P (R_s + R_L)^2}{(\omega M)^2} \right)} \tag{15}$$

Fig. 11 depicts the construction of the Series-Parallel (SP) and Parallel-Parallel (PP) topologies, which exist in addition to the SS topology [59]. The parameter calculation is the same as for the SS topology, and it is defined in Tables 7, 8, and 9 [60].

B. DYNAMIC WIRELESS CHARGING SYSTEM FOR EV (D-WCSEV)

The dynamic model of the wireless charging mode presents the case where the vehicle is charged 8even in motion on the road. The dynamism of the charging mode increases the

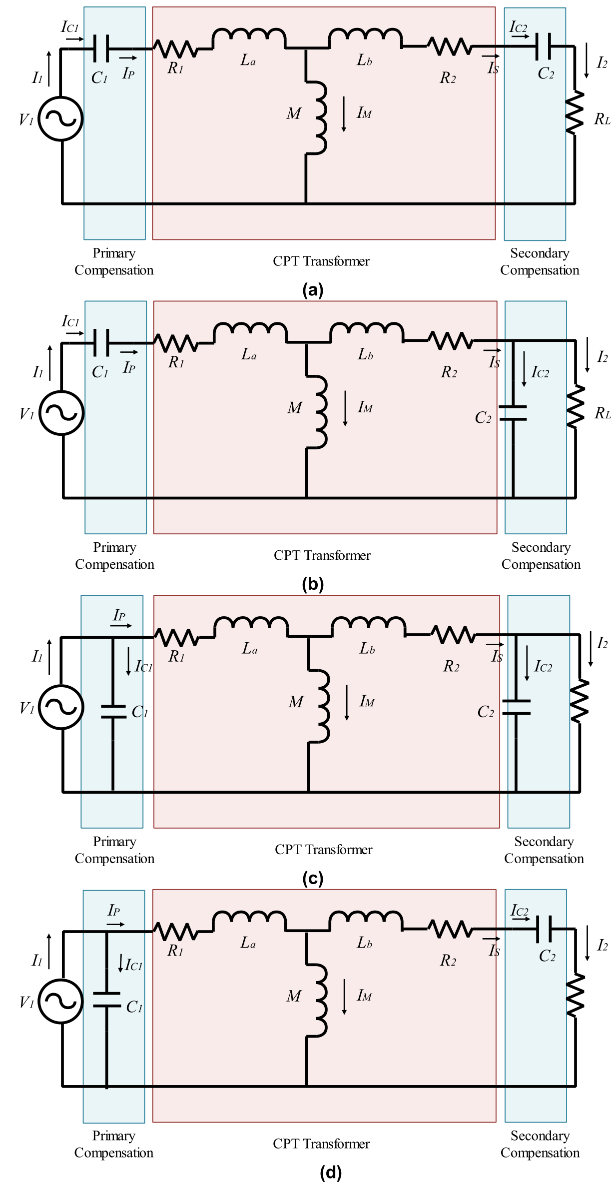

FIGURE 11. Compensation topologies: (a) SS, (b) SP, (c) PP, (d) PS.

TABLE 7. Expressions for the first and secondary capacitors using different topologies.

Topology	Equations
SS topology	$C_1 = \frac{(L_b+M)C_2}{(L_a+M)}$
SP topology	$C_1 = \frac{(L_b+M)^2C_2}{(L_a+M)(L_b+M)-M^2}$
PS topology	$C_1 = \frac{(L_a+M)(L_b+M)^2{C_2}^2{R_L}^2}{M^4+(L_a+M)(L_b+M){R_L}^2}$
PP topology	$C_1 = \frac{(L_b+M)^2((l_a+M)(L_b+M)-M^2)C_2}{((L_b+M)(L_a+M)-M^2)^2+M^4{R_L}^2(L_b+M)C_2}$

Note: C_1=C_2=Cp= Cs.

complexity of its mathematical model and topology as the vehicle's speed parameters are considered due to the vehicle's movement. This results in a complex mathematical model which will expose the obtained power as a function of the

TABLE 8. Efficiency, maximum efficiency, and quality factors expressions for SS and PS topologies [59].

Description	SS	PS
Efficiency	$\eta = \frac{R_L}{(R_L+R_2)\left(1+\frac{R_L(R_2+R_L)}{\omega^2M^2}\right)}$	
Maximum efficiency/ conditions	$\eta_{max} = \frac{R_L}{R_L+R_2}$	$\omega \gg \frac{\sqrt{R_1(R_2+R_L)}}{M}$
Primary and secondary quality factors	$Q_1 = \frac{(L_a+M)R_L}{\omega_0 M^2}$	$Q_2 = \frac{\omega_0(L_b+M)}{R_L}$

Note: R_1=Rp, R_2=Rs.

TABLE 9. Efficiency, maximum efficiency, and quality factors expressions for SP and PP topologies [59].

Description	SP	PP
Efficiency	$\eta = \frac{R_L}{\left(R_L+R_2+\frac{R_2{R_L}^2}{\omega^2(L_b+M)^2}+\frac{R_1{R_2}^2}{\omega^2M^2} + \frac{R_1\left((L_b+M)\omega^2+\frac{R_2R_L}{\omega^2(L_b+M)}\right)^2}{\omega^2M^2}\right)}$	
Maximum efficiency/ conditions	$\eta_{max} = \frac{R_L}{\left(R_L+R_2 + \frac{R_1(L_b+M)^2}{M^2}\right)}$	$\omega \gg \frac{\sqrt{\left(R_2{R_L}^2M^2 + R_1{R_2}^2(L_b+M)^2\right)}}{(L_b+M)M}$
Primary and secondary quality factors	$Q_1 = \frac{\omega_0(L_a+M)(L_b+M)^2}{M^2R_L}$	$Q_2 = \frac{R_L}{\omega_0(L_b+M)}$

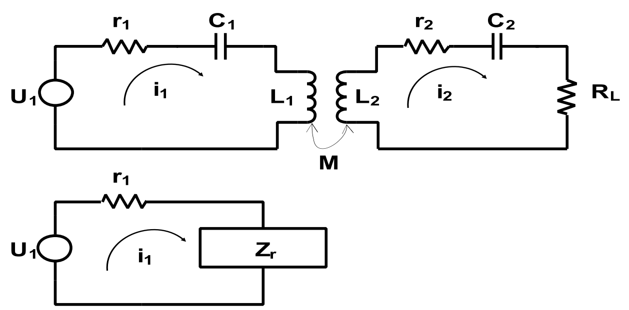

FIGURE 12. The simplified inductive power transfer circuit.

vehicle speed, the parameters of the coil, and the selected compensation topology. Two versions exist for this situation related to the form of the transmitter coil's position and conditions [13], [64].

1) A PRIMARY MODELING METHOD

The first mathematical presentation of the D-WCSEV dynamic model was defined in [20], [56]. The authors used the coupler design, and the choice of operating frequency, which are explained in Fig.12, [65], [66].

It is possible to combine the primary and the secondary coil into a new impedance noted Z_r as in Fig. 12. Then, all the necessary parameters needed to calculate the efficiency of this system can be expressed by Eq. (16) to Eq. (21).

$$\begin{cases} \omega_0 = \frac{1}{\sqrt{LC}} \\ M = K\sqrt{L_1L_2} = kL \end{cases} \tag{16}$$

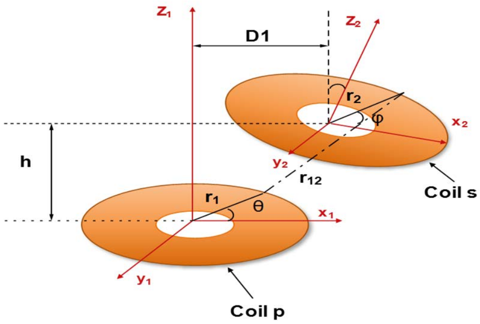

FIGURE 13. Position map of two-wired rings in space.

$$\begin{cases} Z_r = \dfrac{\omega^2 M^2}{(r_2 + R_L)} \\ R_L = \dfrac{U_{out}^2}{P_{out}} \end{cases} \tag{17}$$

$$\begin{cases} P_{out} = |i_2|^2 R_L \\ P_2 = |i_2|^2 (r_2 + R_L) \end{cases} \tag{18}$$

The efficiency of the second and first parts can be calculated in Eq. (19) and (20), respectively. The overall efficiency is given by Eq. (21).

$$\eta_2 = \frac{P_{out}}{P_2} \tag{19}$$

$$\eta_1 = \frac{P_2}{P_1} \tag{20}$$

$$\eta = \eta_1 \eta_2 = \frac{R_L}{(r_2 + R_L)\left[1 + \frac{r_1(r_2+R_L)}{\omega^2 M^2}\right]} \tag{21}$$

2) A SECONDARY MODELING METHOD

Typically, there is a horizontal offset and varied height in wireless EV charging [67]. These issues might reduce the system's efficiency and create power fluctuations. As a result, optimizing EV wireless charging equipment entails resolving these challenges. Fig. 13 depicts the actual position of two coils in space, and Eq. (22) is used to define the new expression of the mutual inductance of the two coils [68]–[70].

$$M = \frac{\mu_0 r_1 r_2}{4\pi} \oiint \left[\frac{\sin\theta \sin\varphi \cos\alpha + \cos\theta \cos\varphi}{r_{12}}\right] d\theta d\varphi \tag{22}$$

where,

$$\begin{cases} r_{12} = [G + H + F]^{1/2} \\ G = r_1^2 + r_2^2 + h^2 + D1^2 - 2hr_2 \cos\varphi \sin\alpha \\ H = 2D1r_2 \cos\varphi \cos\alpha - 2D1r_1 \cos\theta \\ F = -2r_1 r_2 (\cos\theta \cos\varphi \cos\alpha + \sin\theta \sin\varphi) \end{cases} \tag{23}$$

If α, φ, and θ parameters are not varying, Eq. (24) can be used to express the new mutual inductance. Thus, *D1* is a variable according to the receiver's motion face to the transmitter.

$$M = \frac{\mu_0 r_1 r_2}{4\pi} \oiint \left[\frac{1}{r_{12}}\right] d\theta d\varphi \tag{24}$$

where,

$$r_{12} = \sqrt{r_1^2 + r_2^2 + h^2 + D1^2 + 2D1r_2 - 2D1r_1 - 2r_1 r_2} \tag{25}$$

Hence, Eq. (26) and (27) are the new expressions for power and the efficiency of the energetic yields, respectively.

$$P_{wr} = \frac{V_1^2.\omega^2}{Z_{La}.^2 R_L}.\left(\frac{\mu_0 r_1 r_2}{4\pi} \oiint \left[\frac{1}{r_{12}}\right] d\theta d\varphi\right)^2 \tag{26}$$

$$\eta = \frac{R_L}{R_L + R_s + \left[\frac{R_p.(R_s+R_L)^2}{\left(\omega.\left(\frac{u_0 r_1 r_2}{4\pi} \oiint \left[\frac{1}{r_{12}}\right] d\theta d\varphi\right)\right)^2}\right]} \tag{27}$$

C. PROPOSED GENERAL MATHEMATICAL MODEL FOR DS-WCSEV

In this subsection, we propose a new general mathematical model that describes and evaluates the efficiency of both dynamic and static wireless charging systems for EVs (DS-WCSEV). The proposed model works perfectly when the EV is in a dynamic mode (moving on the road) or in a stationary mode (parked). This new mathematical model combines the two previous wireless charging systems, S-WCSEV and D-WCSEV. In this model, all the previously cited parameters and variables for both S-WCSEV and D-WCSEV are considered. The new model takes into account the vehicle speed, the coils size, and electrical parameters and considers any misalignment cases. The shape of the coils, as well as the distance between the transmitter and the receiver, are also taken into account [71]. Eq. (28) to (31) expose all the necessary expressions that evaluate this wireless charging system.

1) MATHEMATICAL MODEL OF THE DS-WCSEV

To begin, the flux relationship between the two receiver and transmitter coils is suggested in Eq. (28). The coefficient presents the percentage of transferred flux from the emitter to the receiver. It is determined by the quantity of the parameter *D1* as shown in Fig. 8. The expression of ϕ_1 is given by Eq. (29). Generally speaking, is between 0 and 1, and it is closely related to the *D1* value as it is presented in Eq. (30).

$$\phi_2 = \beta \cdot \phi_1 \tag{28}$$

$$\phi_1(t) = L_1 i_1(t) + M i_2(t) \tag{29}$$

$$\begin{cases} 0 < \beta < 1 & \text{if } 0 < D1 < coilradius \\ \beta = 1 & \text{if } D1 = 0 \\ \beta = 0 & \text{if } D1 > coilradius \end{cases} \tag{30}$$

The exact expression of, on the other hand, is dependent on the duration of flux transmission, denoted by $T_{transfer}$ and presented in Eq. (31). Where D_{coil} is the coil diameter, and S_p is the vehicle's speed. For the static mode, $S_p \neq 0$, and the transmission time will be endless [72]. ∂ is constant, which is equal to 10^{-5}, μ is constant and equal to 3600.

$$T_{transfer} = \left(\frac{\partial D_{coil}}{S_p}\right)\mu \tag{31}$$

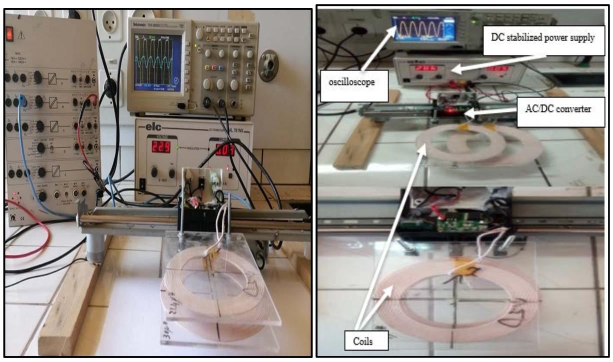

FIGURE 14. Physical material for the wireless power transfer system.

where,

$$\begin{cases} \beta = sin^2\left(\frac{2\pi}{T_{transfer}}t\right) \\ t\epsilon\left[0, T_{transfer}\right] \end{cases} \tag{32}$$

As a result, the voltage output on the secondary coil is defined as in Eq. (33). By multiplying $V_2(t)$ by the number of coil receivers (n_c), Eq. (34) is obtained.

$$\begin{cases} V_2(t) = \beta\left(R_s i_1(t) + L_p \frac{di_1(t)}{dt}\right) + M\frac{di_1(t)}{dt} \\ L_1(\mu H) = \frac{r^2N^2}{8r+\pi\omega} \end{cases} \tag{33}$$

$$\begin{cases} V_{2nc}(t) = n_c V_2(t) \\ P_2(t) = V_{2nc}(t)\cdot i_2(t) \end{cases} \tag{34}$$

2) EXPERIMENTAL VALIDATION

To validate our proposed mathematical model, practical experiments and tests are conducted using a real prototype that we have built-in our laboratory, as presented in Fig.14. To prevent the risk of instability, the terminals of each transmitter module are coupled in parallel to the filter output through an AC bus line composed of an aluminum bar [12], [18]. Several tests are done for both static and dynamic operation modes. Results demonstrate the validity of our proposed mathematical model, as shown in Tables 10 and 11. Tables 10 and 11 present the real power values measured within the experimental test in our laboratory and the estimated values using our proposed mathematical model from Eq. (28) to (34). Results show that the error is about 2% for the worst case. The same situation is validated for the dynamic operation mode, where the error is also minimal. Table 11 shows the dynamic mode operation results. We have supposed that the vehicle will pass through 26 transmitted coils, and we have evaluated the given power via the used mathematical model and via practice results. We have obtained 11.55 W using the simulation model and 11.63 W using the real prototype, as in Fig. 14. Some figures in Table 11 show the transmitter's position facing the receiver and the given voltage form in the measurement instrument in the same table.

TABLE 10. Real and simulated values for the static mode operation.

Distance between coils (mm)	Estimated value (Simulation)		Real value (Experimental)	
	Power (W)	Efficiency (%)	Power (W)	Efficiency (%)
10	47	97	46.2	96
70	31	64	29.9	60
100	24	50	24.3	50
150	18	37	17.8	33

D. FULL RESONANT SYSTEM AND CONTROL

In general, to improve the WPT, two factors must be considered. The first is the inverter control frequency f_s, which must be well controlled and regulated for the inverter to work at resonance ($f_s = f_0$), therefore, allowing maximum power transfer. Changes in Inductively Coupled Transformer (ICT) settings for different coupling instances will modify the system's overall resonant frequency. Aside from frequency regulation, which is done with a constant input voltage in mind, the output power must also be controlled. The power in the entire system is regulated by operating on the input voltage. This outer loop, which is slower than the internal frequency regulation loop, is not addressed in our research. The Maximum Power Point Tracking (MPPT) approach is no longer widely employed in WPT systems. The authors of [73], [74] developed a circuit for using the MPPT regime to regulate the IPT frequency while the car is moving. In this example, an MPPT algorithm is incorporated into MATLAB and implemented without being tied to a specific circuit. Furthermore, while the authors of [75] acknowledged the MPPT approach for frequency management, their controller is not described [55]. Fig. 15 depicts a generally closed-loop system, and Fig. 16 depicts the frequency regulation loop in detail. However, there is another way to simplify this MPPT technique for our frequency regulation in [44]. The goal is to get feedback from the system's DC input, as it is always done in a photovoltaic system when the MPPT process is used, as shown in Fig. 16. The DC input power applied to the MPPT algorithm is calculated using the input DC voltage U_i and the current of the DC input I_i. Fig. 16 depicts the simulation of a case for the entire IPT system utilizing closed-loop control. In this scenario, the EV's reference position ($d = 0.15$m, $s_h = 0$) was taken into account, and the needed power for the load is 3 kW. As a result, the resonant frequency that maximizes transferred power is $f_0 = 30$kHz. The frequency determined by the controller should be equal to f_0. The inverter's duty cycle is D = 0.5, and the load is the battery model depicted in Fig. 16. The fluctuation range is defined by the lower and upper limit frequencies [25 kHz, 35 kHz]. As a result, all potential k scenarios for frequency regulation are included in this frequency spectrum.

IV. COMPARISON OF DIFFERENT MODELS IN RESEARCH

In this paper, we show several mathematical models of wireless charging systems. The best choice of the mathematical model can be related to simplicity and efficiency. The given

TABLE 11. Real and estimated values for the dynamic mode operation.

	Simulation	Experimental validation
Expression β (equation (32))	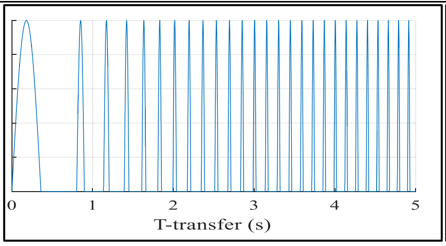	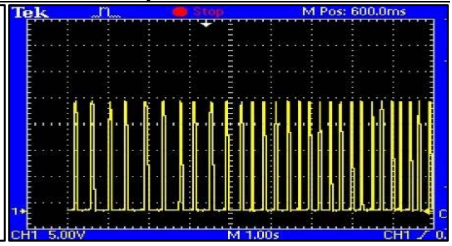
	$\sum P = 11.55W$	$\sum P = 11.63W$
Coils Position		
Position 1 (D1=0)	**Positio 2 (D1=125mm)**	**Position 3 (D1=220mm)**
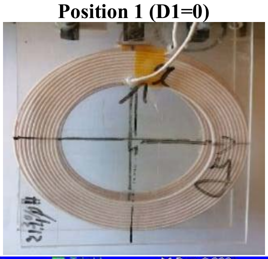	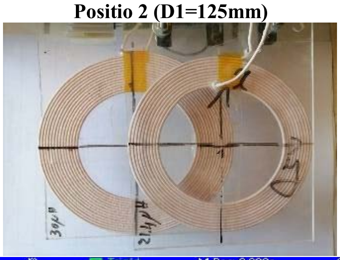	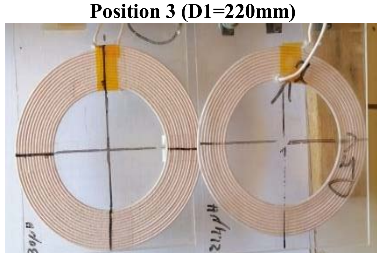
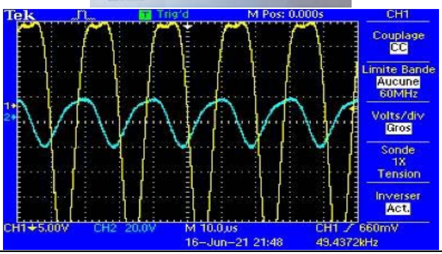	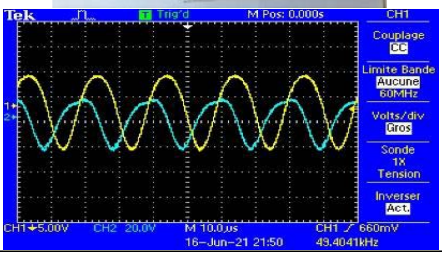	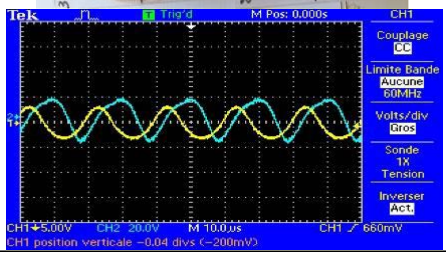

$\sum P$: Average Power Value

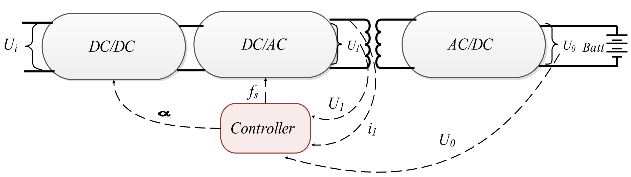

FIGURE 15. Closed-loop for an IPT system with frequency and power controllers.

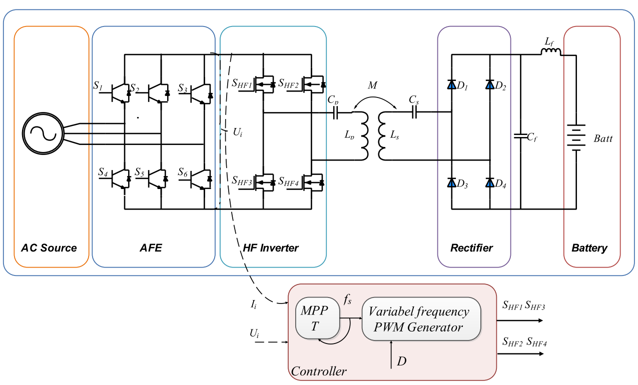

FIGURE 16. Closed-loop for an IPT system with a frequency controller by MPPT.

statistics prove the best choice too. Based on other research papers and our proposed model in this paper, we evaluate and compare the three chosen mathematical models, S-WCSEV, D-WCSEV, and DS-WCSEV, as in Table 12. A production review of D-WCSEV and S-WCSEV has been demonstrated in Tables 13, 14, and 15, [13], [64]–[66], [68], [69].

TABLE 12. Comparison between three mathematical models.

	Complexity	Efficiency	Most used	Usage rate
S-WCSEV	Medium	Medium	High	↓
D-WCSEV	High	Low	Medium	↓
DS-WCSEV	Low	High	Low	↑

V. FUTURE APPLICATION CONCEPTS OF WPT

A. WIRELESS VEHICLE TO GRID (W-V2G)

Fig. 17 depicts the introduction of a wireless V2G to feed the grid. Unlike plug-in V2G, the major site of the wireless transformer is implanted on the road or parking surface with bidirectional power converters. The receiver coil is situated beneath the car, and the remaining bidirectional power converters are mounted in the vehicle's body. The architecture is completely self-contained and provides additional insulation between the source and receiver sides via the wireless transformer. The architecture enables surplus energy to be supplied to EVs to reduce stress or obtain energy in static or dynamic modes to remedy peak demand energy. In addition, in a dynamic V2G service, this technology can

TABLE 13. A synopsis of the study and development of (D-WCSEV).

Research and Development	Operating Frequency (kHz)	Pick-up Power (kW)	Air-gap (mm)	Efficiency (%)	Ref.
Oak Ridge National Laboratory (ORNL)	22–23	125–175	20	90	[76]
Japan Railway Technical Research Institute	10	50	7.5	TBA	[77]
University of Auckland, New Zealand	12.9	20–30	500	85	[57], [78]
Flanders Drive with industries and universities	20	80	100	88–90	[79]
EV System Lab & Nissan Research Centre	90	1	100	>90	[80]
North Carolina State University, USA	100	0.3	170	77–90	[81]
KAIST University, Korea	20	3	10	72–80	[79], [82]

TABLE 14. Development in stationary wireless charging systems (S-WCSEV).

Research /Development	Vehicle type	Air-gap (mm)	Frequency (kHz)	Power (kW)	Efficiency (%)	Ref.
Companies and Start-Up (Industries)						
Siemens and BMW	Car	80-160	TBA	3.8	>90	[83]
Delphi	Car	200	TBA	3.4	TBA	[84]
Conductix-Wampfler	Industry fleet and Bus	TBA	20	Up to 20	TBA	[85]
Witricy corporation	Passenger cars and SUVs	160-220	85	3.6	>90	[86]
Groups Research and Universities						
Wuhan University, China	Lab Exp	300	100	6-16	>81	[87]
Michigan State University	Lab Exp	200	60	1	95-96	[88]
University og Michigan Dearborn	Lab Exp	200	TBA	8	95.7	[89]
The University of Georgi	Lab Prot	160	20	3	>80	[90]

TABLE 15. Research and development of dynamic and stationary wireless charging systems are summarized (DS-WCSEV).

Research and Development	Operating Frequency (kHz)	Pick-up Power (kW)	Air-gap (mm)	Efficiency (%)	Ref.
Department of Industrial Systems Engineering, Korea	10-17	5-40	18	84	[91]
Department of Electrical and Computer Engineering University, Miami	40	70	12	78	[92]
University of Gabes Tunisia	50	8	15	90	[93]
Oak Ridge National Laboratory	20	3	100	>90	[94]

serve as a buffer or backup for mobile energy storage [95]. Table 16 proves the comparison of wireless V2G vs. plug-in V2G.

B. INTEGRATION WITH RENEWABLE ENERGY

Using typical wireless charging techniques, alternating electricity from non-renewable sources was employed as the device input. The alternating value is then rectified to DC for high-frequency inverters. Engineers have begun using solar electricity for energy in automotive parking lots and pavements for static and dynamic charging. In addition to saving energy, this can reduce the complexity, size, and failure of the entire charging station circuit by eliminating the full rectifier block. Renewable energy types such as solar, wind, and others can be stored in batteries and utilized to charge EVs in DC format using a wireless charging system, as shown in Figure 17. In 2015, this scheme was suggested in a paper by Vithayasrichareon *et al.* [96]. The paper [97] released in the same year described the experimental set-up of a solar-powered wireless charging prototype. But they showed some significant disadvantages for both papers, such as high input current, low performance, and lower transfer efficiency for both SS and LLC topologies [98]. So, both of them were concentrating on a charging device for a set distance. And in 2020, on its campus, Delft University launched a solar-powered bicycle charging station, the first of its kind [99]. Another disadvantage was the incorporated pseudo-wireless charging kickstand, as well as the lower performance. The lack of an input current ripple mitigation device resulted in severe ohmic losses in both situations, necessitating a large coil value for the transmitter and receiver. Furthermore, the receiver position resulted in a large leakage flow to the bicycle's body. As a result, a novel wireless charger powered by renewable energy can be created using an optimal input filter design and carefully constructed transmitter and receiver coils with adequate mutual inductance.

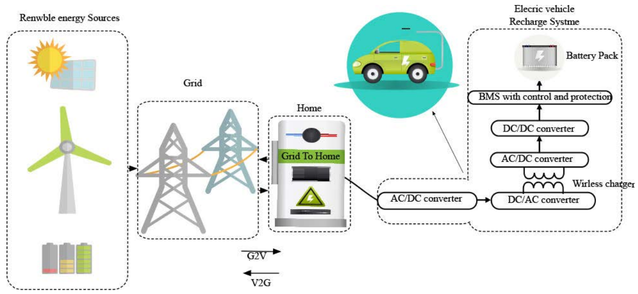

FIGURE 17. Bidirectional power transfer applications for wireless charging systems, including renewable energy sources.

TABLE 16. Comparison of wireless V2G vs plug-in V2G.

Features	Wireless V2G	Plug-In V2G
Method	Wireless power transfer	Traditional method
Operating frequency	79.9-9-88kHz	15-100 kHz
Power Transfer Efficiency	>89%	>89%
Air-gap sensitivity	Medium-High	N/A
Power transfer capability	High	High
Power transfer scheduling	Automatic	Manual
Convenience	Very high	Medium

C. WIRELESS POWER TRANSFER IN THE SPACE SECTOR: ORBITAL SOLAR POWER PLANTS

An orbital solar power plant involves placing solar panels in space at an altitude of approximately 36,000 kilometers (Fig. 18). This location would allow photovoltaic cells to

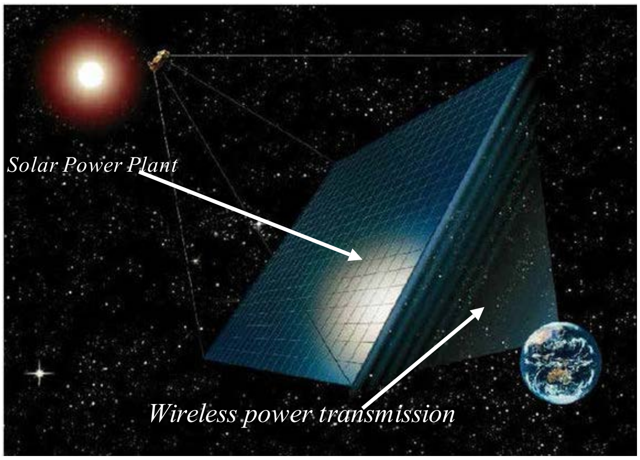

FIGURE 18. Functional diagram of an orbital solar power plant.

absorb a large amount of solar irradiance at all times and thus obtain optimum performance. This project was planned over forty years ago by the famous scientist Peter Glaser. This idea has been analyzed by NASA and the European Space Agency. Research from these institutions confirms the feasibility of this project, the only existing barrier being economical. The Japanese space agency, JAXA, has been working since 1998 to launch a prototype solar power plant in geostationary orbit and hopes for a launch in 2040 [100]. Given that the sun's life expectancy is estimated at 5 billion years, we can say that the wireless transmission of electricity from space could revolutionize our transport habits and encourage the development of new technologies as well as complete the current network. Apart from that, one cannot deny the difficulties which govern this technology. The assembly of the solar panels requires a large number of rocket launches which poses an economic barrier.

D. WIRELESS POWER TRANSFER IN THE MEDICAL FIELD

The recharging and operation of various devices and devices remotely represent a great interest in the medical field. Certain implanted medical devices require a high level of power for their operations, especially in the transcutaneous transfer in cardiac battery systems. This is why it is interesting to replace traditional magnetic induction, which allows efficient transfer of energy. This energy capture device can be implanted deep into the body cavity, several inches below the skin. Likewise, the energy source can be several centimeters from the surface of the skin, facilitating, in particular, the installation of ventricular assistance devices, cardiac pacemakers, defibrillators, the restoration of the motor functions of organs affected as a result of an accident or an illness, stimulation of the muscles, and alleviation of the effects of certain types of illness (Visual prostheses used to restore vision loss, diagnosis of the gastrointestinal tract, etc.) [101], [102]. The use of cardiac assist devices, for example, to bypass ventricular dysfunctions is beneficial. Conventional methods of supply, on the other hand, may pose additional risks associated with the development of infections when threads are passed through the skin. To address this issue, a new resonant converter with a coreless transformer was developed, allowing for the provision of a prototype of such a cardiac assist device. The transferred power is 10 W, and the operating frequency is 205.1 kHz [103]. Transcutaneous energy transfer is also intended for use in the creation of an implanted mechanical heart. The primary coil must be placed near the secondary coil to have a good connection. The coreless transformer is made up of two circular spiral coils held together by amorphous radial fibers. These fibers provide flexibility to the coils and contain magnetic elements that are thought to assist energy transfer by focusing the flux through the coils. Transcutaneous energy transfer is used to deliver electrodes to generate electrical stimulation to restore movement to paralyzed limbs caused by a spinal cord injury. The primary coil is shaped like a solenoid and is wrapped around the limb. Secondary coils with spiral forms are connected to electrodes. To obtain a portable and autonomous implantable system, the electronic circuits of the implant must be small and consume little power. The most important aspect in the design of electronic implants in the biomedical field is therefore the energy supply [103]. The system is mainly composed of a part going into the human body (internal unit) and an external control unit or external controller, as shown in Fig. 19, [104].

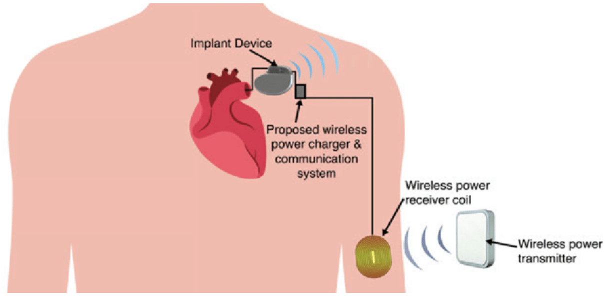

FIGURE 19. Example of application in the medical field: Explanatory diagram of a pacemaker.

VI. CONCLUSION

This paper summarizes different wireless charging system topologies that can be used for EV applications. It starts with a short overview of EV architectures and cites some statistics regarding the usage of wireless charging systems in industries. Also, it presents different coil shapes, mathematical models, different architectures, and topologies of the WPT for both dynamic (EV is moving) and static (EV is parked) modes. In addition, this paper shows all the essential parameters and variables that help in building a solid mathematical model for the wireless charging system. Moreover, the authors of this work propose a new general mathematical model that can work for both dynamic and static modes with high accuracy. For validation purposes of the proposed mathematical model, a real prototype was built in our laboratory in which the results from experiments confirm the validity of our proposed model with a small error margin. Finally, future application concepts of the WPT were presented and discussed in which the deployment of WPT systems is possible when it is coupled with renewable energy systems.

ACKNOWLEDGMENT

This work was supported and funded by Taif University Researchers Supporting Project Number TURSP-2020/34, Taif University, Taif, Saudi Arabia.

REFERENCES

[1] N. Mohamed, F. Aymen, Z. M. Ali, A. F. Zobaa, and S. H. E. A. Aleem, "Efficient power management strategy of electric vehicles based hybrid renewable energy," *Sustainability*, vol. 13, no. 13, p. 7351, Jun. 2021, doi: 10.3390/su13137351.

[2] A. Ahmad, Z. A. Khan, and M. S. Alam, "A review of the electric vehicle charging techniques, standards, progression and evolution of EV technologies in Germany," *Smart Sci.*, vol. 477, pp. 1–18, Jan. 2018, doi: 10.1080/23080477.2017.1420132.

[3] P. García, L. M. Fernández, J. P. Torreglosa, and F. Jurado, "Operation mode control of a hybrid power system based on fuel cell/battery/ultracapacitor for an electric tramway," *Comput. Electr. Eng.*, vol. 39, no. 7, pp. 1993–2004, Oct. 2013, doi: 10.1016/j.compeleceng.2013.04.022.

[4] A. Trivino-Cabrera, M. Ochoa, D. Fernandez, and J. A. Aguado, "Independent primary-side controller applied to wireless chargers for electric vehicles," in *Proc. IEEE Int. Electr. Vehicle Conf. (IEVC)*, Dec. 2014, pp. 1–5, doi: 10.1109/IEVC.2014.7056193.

[5] N. Mohamed, F. Aymen, and B. H. Mouna, "Influences of photovoltaics cells number for the charging system electric vehicle," in *Proc. 17th Int. Multi-Conf. Syst., Signals Devices (SSD)*, Jul. 2020, pp. 244–248, doi: 10.1109/ssd49366.2020.9364141.

[6] Y. Wang, Z. Wu, Y. Chen, A. Xia, C. Guo, and Z. Tang, "Research on energy optimization control strategy of the hybrid electric vehicle based on Pontryagin's minimum principle," *Comput. Electr. Eng.*, vol. 72, pp. 203–213, Nov. 2018, doi: 10.1016/j.compeleceng.2018.09.018.

[7] T. M. Fisher, K. B. Farley, Y. Gao, H. Bai, and Z. T. Tse, "Electric vehicle wireless charging technology: A state-of-the-art review of magnetic coupling systems," *Wireless Power Transf.*, vol. 1, no. 2, pp. 87–96, 2014, doi: 10.1017/wpt.2014.8.

[8] N. Mohamed, F. Aymen, Z. Issam, M. Bajaj, and S. S. M. Ghoneim, "The impact of coil position and number on wireless system performance for electric vehicle recharging," *Sensors*, vol. 21, no. 4343, pp. 1–19, 2021, doi: 10.3390/s21134343.

[9] J. Wang, Y. Cai, L. Chen, D. Shi, R. Wang, and Z. Zhu, "Review on multi-power sources dynamic coordinated control of hybrid electric vehicle during driving mode transition process," *Int. J. Energy Res.*, vol. 44, no. 8, pp. 6128–6148, Jun. 2020, doi: 10.1002/er.5264.

[10] A. Triviño, J. M. González-González, and J. A. Aguado, "Wireless power transfer technologies applied to electric vehicles: A review," *Energies*, vol. 14, no. 6, p. 1547, Mar. 2021, doi: 10.3390/en14061547.

[11] N. D. Mazharov, S. M. Hristov, D. A. Dichev, and I. S. Zhelezarov, "Some problems of dynamic contactless charging of electric vehicles," *Acta Polytech. Hungarica*, vol. 14, no. 4, pp. 7–26, 2017, doi: 10.12700/APH.14.4.2017.4.1.

[12] N. Mohamed, F. Aymen, S. Lassaad, and B. H. Mouna, "Practical validation of the vehicle speed influence on the wireless recharge system efficiency," in *Proc. 6th IEEE Int. Energy Conf. (ENERGYCon)*, Sep. 2020, pp. 372–376, doi: 10.1109/energycon48941.2020.9236475.

[13] M. Fuller, "Wireless charging in California: Range, recharge, and vehicle electrification," *Transp. Res. C, Emerg. Technol.*, vol. 67, pp. 343–356, Jun. 2016, doi: 10.1016/j.trc.2016.02.013.

[14] S. Zouaoui, W. Dghais, R. Melicio, and H. Belgacem, "Omnidirectional WPT and data communication for electric air vehicles: Feasibility study," *Energies*, vol. 13, no. 24, p. 6480, Dec. 2020, doi: 10.3390/en13246480.

[15] Z. Bi, L. Song, R. De Kleine, C. C. Mi, and G. A. Keoleian, "Plug-in vs. wireless charging: Life cycle energy and greenhouse gas emissions for an electric bus system," *Appl. Energy*, vol. 146, pp. 11–19, May 2015, doi: 10.1016/j.apenergy.2015.02.031.

[16] P. Cao, Y. Tang, F. Zhu, Z. Zhang, J. Zhou, Z. Bai, and H. Ma, "An IPT system with constant current and constant voltage output features for EV charging," in *Proc. 44th Annu. Conf. IEEE Ind. Electron. Soc. (IECON)*, Oct. 2018, pp. 4775–4780, doi: 10.1109/IECON.2018.8591213.

[17] M. Frivaldsky and M. Pavelek, "In loop design of the coils and the electromagnetic shielding elements for the wireless charging systems," *Energies*, vol. 13, no. 24, p. 6661, Dec. 2020, doi: 10.3390/en13246661.

[18] N. Mohamed, F. Aymen, and A. Mohammed, "Inductive power transmission system for electric car charging phase: Modeling plus frequency analysis," *World Electr. Veh. J.*, vol. 12, no. 4, pp. 1–11, 2021, doi: 10.3390/wevj12040267.

[19] P. A. J. Lawton, F. J. Lin, and G. A. Covic, "Magnetic design considerations for high-power wireless charging systems," *IEEE Trans. Power Electron.*, early access, Feb. 25, 2022, doi: 10.1109/tpel.2022.3154365.

[20] A. Ahmad, M. S. Alam, and R. Chabaan, "A comprehensive review of wireless charging technologies for electric vehicles," *IEEE Trans. Transport. Electrific.*, vol. 4, no. 1, pp. 38–63, Mar. 2018, doi: 10.1109/TTE.2017.2771619.

[21] K. A. Kalwar, S. Mekhilef, M. Seyedmahmoudian, and B. Horan, "Coil design for high misalignment tolerant inductive power transfer system for EV charging," *Energies*, vol. 9, no. 11, pp. 12–17, 2016, doi: 10.3390/en9110937.

[22] J. L. Villa, J. Sallan, J. F. S. Osorio, and A. Llombart, "High-misalignment tolerant compensation topology for ICPT systems," *IEEE Trans. Ind. Electron.*, vol. 59, no. 2, pp. 945–951, Feb. 2012, doi: 10.1109/TIE.2011.2161055.

[23] N. Mohamed, F. Aymen, B. H. Mouna, and S. Alassaad, "Review on autonomous charger for EV and HEV," in *Proc. Int. Conf. Green Energy Convers. Syst. (GECS)*, Mar. 2017, pp. 1–6, doi: 10.1109/GECS.2017.8066273.

[24] G. A. Covic and J. T. Boys, "Modern trends in inductive power transfer for transportation applications," *IEEE J. Emerg. Sel. Topics Power Electron.*, vol. 1, no. 1, pp. 28–41, Mar. 2013, doi: 10.1109/JESTPE.2013.2264473.

[25] S. Y. R. Hui, W. Zhong, and C. K. Lee, "A critical review of recent progress in mid-range wireless power transfer," *IEEE Trans. Power Electron.*, vol. 29, no. 9, pp. 4500–4511, Sep. 2014.

[26] A. F. A. Aziz, M. F. Romlie, and Z. Baharudin, "Review of inductively coupled power transfer for electric vehicle charging," *IET Power Electron.*, vol. 12, no. 14, pp. 3611–3623, Nov. 2019, doi: 10.1049/iet-pel.2018.6011.

[27] S. Li and C. C. Mi, "Wireless power transfer for electric vehicle applications," *IEEE J. Emerg. Sel. Topics Power Electron.*, vol. 3, no. 1, pp. 4–17, Mar. 2015, doi: 10.1109/JESTPE.2014.2319453.

[28] T. W. Ching and Y. S. Wong, "Review of wireless charging technologies for electric vehicles," in *Proc. 5th Int. Conf. Power Electron. Syst. Appl. (PESA)*, Dec. 2013, pp. 24–27, doi: 10.1109/PESA.2013.6828235.

[29] Y. Ota, H. Taniguchi, T. Nakajima, K. M. Liyanage, J. Baba, and A. Yokoyama, "Autonomous distributed V2G (vehicle-to-grid) satisfying scheduled charging," *IEEE Trans. Smart Grid*, vol. 3, no. 1, pp. 559–564, Mar. 2012, doi: 10.1109/TSG.2011.2167993.

[30] F. Musavi and W. Eberle, "Overview of wireless power transfer technologies for electric vehicle battery charging," *IET Power Electron.*, vol. 7, no. 1, pp. 60–66, Jan. 2014, doi: 10.1049/iet-pel.2013.0047.

[31] C. Liu, A. P. Hu, B. Wang, and N.-K. C. Nair, "A capacitively coupled contactless matrix charging platform with soft switched transformer control," *IEEE Trans. Ind. Electron.*, vol. 60, no. 1, pp. 249–260, Jan. 2013, doi: 10.1109/TIE.2011.2172174.

[32] J. Dai and D. C. Ludois, "Capacitive power transfer through a conformal bumper for electric vehicle charging," *IEEE J. Emerg. Sel. Topics Power Electron.*, vol. 4, no. 3, pp. 1015–1025, Sep. 2016, doi: 10.1109/JESTPE.2015.2505622.

[33] A. P. Hu, C. Liu, and H. L. Li, "A novel contactless battery charging system for soccer playing robot," in *Proc. 15th Int. Conf. Mechatronics Mach. Vis. Pract.*, Dec. 2008, pp. 646–650, doi: 10.1109/MMVIP.2008.4749606.

[34] D. C. Ludois, M. J. Erickson, and J. K. Reed, "Aerodynamic fluid bearings for translational and rotating capacitors in noncontact capacitive power transfer systems," *IEEE Trans. Ind. Appl.*, vol. 50, no. 2, pp. 1025–1033, Mar./Apr. 2014, doi: 10.1109/TIA.2013.2273484.

[35] J. Kim and F. Bien, "Electric field coupling technique of wireless power transfer for electric vehicles," in *Proc. IEEE Tencon-Spring*, Apr. 2013, pp. 267–271, doi: 10.1109/TENCONSpring.2013.6584453.

[36] H. Jiang, J. Zhang, D. Lan, K. K. Chao, S. Liou, H. Shahnasser, R. Fechter, S. Hirose, M. Harrison, and S. Roy, "A low-frequency versatile wireless power transfer technology for biomedical implants," *IEEE Trans. Biomed. Circuits Syst.*, vol. 7, no. 4, pp. 526–535, Aug. 2013, doi: 10.1109/TBCAS.2012.2220763.

[37] P. K. Joseph, E. Devaraj, and A. Gopal, "Overview of wireless charging and vehicle-to-grid integration of electric vehicles using renewable energy for sustainable transportation," *IET Power Electron.*, vol. 12, no. 4, pp. 627–638, Apr. 2019, doi: 10.1049/iet-pel.2018.5127.
[38] B. Minnaert, F. Mastri, M. Mongiardo, A. Costanzo, and N. Stevens, "Constant capacitive wireless power transfer at variable coupling," in *IEEE MTT-S Int. Microw. Symp. Dig.*, May 2018, pp. 1–4, doi: 10.1109/IEEE-IWS.2018.8400878.
[39] H.-D. Lang, A. Ludwig, and C. D. Sarris, "Convex optimization of wireless power transfer systems with multiple transmitters," *IEEE Trans. Antennas Propag.*, vol. 62, no. 9, pp. 4623–4636, Sep. 2014, doi: 10.1109/TAP.2014.2330584.
[40] D. Ustun, S. Balci, and K. Sabanci, "A parametric simulation of the wireless power transfer with inductive coupling for electric vehicles, and modelling with artificial bee colony algorithm," *Measurement*, vol. 150, Jan. 2020, Art. no. 107082, doi: 10.1016/j.measurement.2019.107082.
[41] S. Wang, D. G. Dorrell, Y. Guo, and M. F. Hsieh, "Inductive charging coupler with assistive coils," *IEEE Trans. Magn.*, vol. 52, no. 7, pp. 10–13, Mar. 2016, doi: 10.1109/TMAG.2016.2539340.
[42] Y. Shi, Y. Zhang, M. Shen, Y. Fan, C. Wang, and M. Wang, "Design of a novel receiving structure for wireless power transfer with the enhancement of magnetic coupling," *AEU-Int. J. Electron. Commun.*, vol. 95, pp. 236–241, Oct. 2018, doi: 10.1016/j.aeue.2018.08.033.
[43] J. H. Kim, B.-S. Lee, J.-H. Lee, S.-H. Lee, C.-B. Park, S.-M. Jung, S.-G. Lee, K.-P. Yi, and J. Baek, "Development of 1-MW inductive power transfer system for a high-speed train," *IEEE Trans. Ind. Electron.*, vol. 62, no. 10, pp. 6242–6250, Oct. 2015, doi: 10.1109/TIE.2015.2417122.
[44] N. Mohamed, F. Aymen, M. Alqarni, R. A. Turky, B. Alamri, Z. M. Ali, and S. H. E. A. Aleem, "A new wireless charging system for electric vehicles using two receiver coils," *Ain Shams Eng. J.*, vol. 13, no. 2, Mar. 2022, Art. no. 101569, doi: 10.1016/j.asej.2021.08.012.
[45] M. Yilmaz and P. T. Krein, "Review of battery charger topologies, charging power levels, and infrastructure for plug-in electric and hybrid vehicles," *IEEE Trans. Power Electron.*, vol. 28, no. 5, pp. 2151–2169, May 2013, doi: 10.1109/TPEL.2012.2212917.
[46] Z. Bi, T. Kan, C. C. Mi, Y. Zhang, Z. Zhao, and G. A. Keoleian, "A review of wireless power transfer for electric vehicles: Prospects to enhance sustainable mobility," *Appl. Energy*, vol. 179, pp. 413–425, Oct. 2016, doi: 10.1016/j.apenergy.2016.07.003.
[47] K. A. Kalwar, M. Aamir, and S. Mekhilef, "Inductively coupled power transfer (ICPT) for electric vehicle charging—A review," *Renew. Sustain. Energy Rev.*, vol. 47, pp. 462–475, Jul. 2015, doi: 10.1016/j.rser.2015.03.040.
[48] S. Chopra, "Contactless power transfer for electric vehicle charging application," *Science*, vol. 80, Aug. 2011.
[49] J. Zhao, T. Cai, S. Duan, H. Feng, C. Chen, and X. Zhang, "A general design method of primary compensation network for dynamic WPT system maintaining stable transmission power," *IEEE Trans. Power Electron.*, vol. 31, no. 12, pp. 8343–8358, Dec. 2016, doi: 10.1109/TPEL.2016.2516023.
[50] D. Version, "Design of static wireless charging system for electric vehicles with focus on magnetic coupling and emissions," Ph.D. dissertation, 2015.
[51] X. Shi, C. Qi, M. Qu, S. Ye, G. Wang, L. Sun, and Z. Yu, "Effects of coil shapes on wireless power transfer via magnetic resonance coupling," *J. Electromagn. Waves Appl.*, vol. 28, no. 11, pp. 1316–1324, Jul. 2014, doi: 10.1080/09205071.2014.919879.
[52] A. Ahmad, M. S. Alam, and A. A. S. Mohamed, "Design and interoperability analysis of quadruple pad structure for electric vehicle wireless charging application," *IEEE Trans. Transport. Electrific.*, vol. 5, no. 4, pp. 934–945, Dec. 2019, doi: 10.1109/TTE.2019.2929443.
[53] M. Budhia, G. A. Covic, and J. T. Boys, "Design and optimization of circular magnetic structures for lumped inductive power transfer systems," *IEEE Trans. Power Electron.*, vol. 26, no. 11, pp. 3096–3108, Nov. 2011, doi: 10.1109/TPEL.2011.2143730.
[54] S. Member, G. A. Covic, and J. T. Boys, "Design and optimisation of magnetic structures for lumped inductive power transfer systems," in *Proc. IEEE Energy Convers. Congr. Expo.*, Sep. 2009, pp. 2081–2088.
[55] F. Aymen, N. Mohamed, S. Chayma, C. H. R. Reddy, M. M. Alharthi, and S. S. M. Ghoneim, "An improved direct torque control topology of a double stator machine using the fuzzy logic controller," *IEEE Access*, vol. 9, pp. 126400–126413, 2021, doi: 10.1109/access.2021.3110477.
[56] C. Cai, J. Wang, Z. Fang, P. Zhang, M. Hu, J. Zhang, L. Li, and Z. Lin, "Design and optimization of load-independent magnetic resonant wireless charging system for electric vehicles," *IEEE Access*, vol. 6, pp. 17264–17274, 2018, doi: 10.1109/ACCESS.2018.2810128.
[57] G. A. Covic and J. T. Boys, "Inductive power transfer," *Proc. IEEE*, vol. 101, no. 6, pp. 1276–1289, Jun. 2013, doi: 10.1109/JPROC.2013.2244536.
[58] G. Wang, M. Yang, L. Niu, X. Gui, and D. Xu, "A static current error elimination algorithm for PMSM predictive current control," *Zhongguo Dianji Gongcheng Xuebao, Chin. Soc. Electr. Eng.*, vol. 35, no. 10, pp. 2544–2551, 2015, doi: 10.13334/j.0258-8013.pcsee.2015.10.021.
[59] C.-S. Wang, G. A. Covic, and O. H. Stielau, "Power transfer capability and bifurcation phenomena of loosely coupled inductive power transfer systems," *IEEE Trans. Ind. Electron.*, vol. 51, no. 1, pp. 148–157, Feb. 2004, doi: 10.1109/TIE.2003.822038.
[60] R. Vaka and R. Keshri, "Review on contactless power transfer for electric vehicle charging," *Energies*, vol. 10, no. 5, p. 636, May 2017, doi: 10.3390/en10050636.
[61] G. Rituraj, E. R. Joy, B. K. Kushwaha, and P. Kumar, "Analysis and comparison of series-series and series-parallel topology of contactless power transfer systems," in *Proc. IEEE Region Conf. (TENCON)*, Oct. 2014, pp. 1–6, doi: 10.1109/TENCON.2014.7022440.
[62] M. K. Naik, M. Bertoluzzo, and G. Buja, "Design of a contactless battery charging system," in *Proc. Africon*, Sep. 2013, pp. 1–6, doi: 10.1109/AFRCON.2013.6757758.
[63] T.-D. Nguyen, S. Li, W. Li, and C. C. Mi, "Feasibility study on bipolar pads for efficient wireless power chargers," in *Proc. IEEE Appl. Power Electron. Conf. Expo. (APEC)*, Mar. 2014, pp. 1676–1682, doi: 10.1109/APEC.2014.6803531.
[64] M. Yilmaz and P. T. Krein, "Review of the impact of vehicle-to-grid technologies on distribution systems and utility interfaces," *IEEE Trans. Power Electron.*, vol. 28, no. 12, pp. 5673–5689, Dec. 2013, doi: 10.1109/TPEL.2012.2227500.
[65] R. Maeno, H. Omori, H. Michikoshi, N. Kimura, and T. Morizane, "A 3kW single-ended wireless EV charger with a newly developed SiC-VMOSFET," in *Proc. 7th Int. Conf. Renew. Energy Res. Appl. (ICRERA)*, Oct. 2018, pp. 418–423, doi: 10.1109/ICRERA.2018.8566866.
[66] K. Lee, Z. Pantic, and S. M. Lukic, "Reflexive field containment in dynamic inductive power transfer systems," *IEEE Trans. Power Electron.*, vol. 29, no. 9, pp. 4592–4602, Sep. 2014, doi: 10.1109/TPEL.2013.2287262.
[67] J. Sallan, J. L. Villa, A. Llombart, and J. F. Sanz, "Optimal design of ICPT systems applied to electric vehicle battery charge," *IEEE Trans. Ind. Electron.*, vol. 56, no. 6, pp. 2140–2149, Jun. 2009, doi: 10.1109/TIE.2009.2015359.
[68] K. Hata, T. Imura, and Y. Hori, "Dynamic wireless power transfer system for electric vehicles to simplify ground facilities-sensorless vehicle detection and power control strategy," in *Proc. 30th Int. Electr. Veh. Symp. Exhib. (EVS)*, 2017, pp. 1731–1736.
[69] X. Zhang, Z. Yuan, Q. Yang, Y. Li, J. Zhu, and Y. Li, "Coil design and efficiency analysis for dynamic wireless charging system for electric vehicles," *IEEE Trans. Magn.*, vol. 52, no. 7, pp. 2–5, Feb. 2016.
[70] Y. Guo, J. Li, X. Hou, X. Lv, H. Liang, J. Zhou, and H. Wu, "Poynting vector analysis for wireless power transfer between magnetically coupled coils with different loads," *Sci. Rep.*, vol. 7, no. 1, pp. 1–6, Dec. 2017, doi: 10.1038/s41598-017-00846-w.
[71] L. Tan, J. Li, X. Huang, and C. Xu, "Modeling and analysis of a 3kW wireless charging system for electric vehicle," in *Proc. IEEE PELS Workshop Emerg. Technol., Wireless Power Transf. (WoW)*, May 2017, pp. 189–192, doi: 10.1109/WoW.2017.7959391.
[72] N. Mohamed, F. Aymen, and B. H. Mouna, "Inductive charger efficiency under internal and external parameters variation for an electric vehicle in motion," *Int. J. Powertrains*, vol. 8, no. 4, p. 343, 2019, doi: 10.1504/IJPT.2019.104674.
[73] D. D. Reigosa, F. Briz, C. Blanco, and J. M. Guerrero, "Sensorless control of doubly fed induction generators based on stator high-frequency signal injection," *IEEE Trans. Ind. Appl.*, vol. 50, no. 5, pp. 3382–3391, Sep. 2014, doi: 10.1109/TIA.2014.2303255.
[74] N. Mohamed, F. Aymen, A. Altamimi, and Z. A. Khan, "Power management and control of a hybrid electric vehicle based on photovoltaic, fuel cells, and battery energy sources," *Sustainability*, vol. 14, no. 5, p. 2551, 2022.

[75] V. J. Brusamarello, Y. B. Blauth, R. de Azambuja, I. Müller, and F. R. de Sousa, "Power transfer with an inductive link and wireless tuning," *IEEE Trans. Instrum. Meas.*, vol. 62, no. 5, pp. 924–931, May 2013, doi: 10.1109/TIM.2013.2245041.

[76] R. Walli. (Feb. 27, 2016). *ORNL Surges Forward With 20-Kilowatt Wireless Charging for Vehicles*. [Online]. Available: https://www.ornl.gov/news/ornl-surgesforward-20-kilowatt-wireless-charging-vehicles

[77] H. H. Wu, A. Gilchrist, K. Sealy, and D. Bronson, "A 90 percent efficient 5kW inductive charger for EVs," in *Proc. IEEE Energy Convers. Congr. Expo. (ECCE)*, Sep. 2012, pp. 275–282, doi: 10.1109/ECCE.2012.6342812.

[78] R. H. K. Vatsala, Y. Varshney, and A. Ahmad, "Challenges and potential solutions for the deployment of wireless charging infrastructure for xEVs in India," *Compendium Tech. Papers, Indian Smart Grid Week*, vol. 2017, pp. 55–61, 2017.

[79] K. Hwang, S. Kim, S. Kim, Y. Chun, and S. Ahn, "Design of wireless power transfer system for railway application," *Int. J. Railway*, vol. 5, no. 4, pp. 167–174, Dec. 2012, doi: 10.7782/ijr.2012.5.4.167.

[80] K. Throngnumchai, A. Hanamura, Y. Naruse, and K. Takeda, "Design and evaluation of a wireless power transfer system with road embedded transmitter coils for dynamic charging of electric vehicles," *World Electr. Vehicle J.*, vol. 6, no. 4, pp. 848–857, Dec. 2013, doi: 10.3390/wevj6040848.

[81] K. Lee, Z. Pantic, and S. Lukic, "Field containment in dynamic wireless charging systems through source-reciever interaction," in *Proc. IEEE Energy Convers. Congr. Expo.*, Sep. 2013, pp. 3658–3663, doi: 10.1109/ECCE.2013.6647183.

[82] S. Lee, W. Lee, J. Huh, H.-J. Kim, C. Park, G.-H. Cho, and C.-T. Rim, "Active EMF cancellation method for I-type pickup of on-line electric vehicles," in *Proc. 26th Annu. IEEE Appl. Power Electron. Conf. Expo. (APEC)*, Mar. 2011, pp. 1980–1983, doi: 10.1109/APEC.2011.5744868.

[83] A. Vesco and F. Ferrero, *Handbook of Research on Social, Economic, and Environmental Sustainability in the Development of Smart Cities*. Hershey, PA, USA: IGI Global.

[84] (Sep. 27, 2011). *Delphi Wireless Charging System*. [Online]. Available: http://delphi.com/shared/pdf/ppd/pwrelec/wireless-charging-system.pdf

[85] (Sep. 27, 2014). *Qualcomm Halo Wireless Electric Vehicle Charging*. [Online]. Available: http://www.qualcommhalo.com/index.php/media-centre.html?id=41#media-centre

[86] (Mar. 20, 2017). *Drive: Electric Vehicles*. [Online]. Available: http://witricity.com/ technology/automotive/

[87] Z. Dai, J. Wang, M. Long, and H. Huang, "A witricity-based high-power device for wireless charging of electric vehicles," *Energies*, vol. 10, no. 3, p. 323, Mar. 2017, doi: 10.3390/en10030323.

[88] H. Zeng, S. Yang, and F. Z. Peng, "Design consideration and comparison of wireless power transfer via harmonic current for PHEV and EV wireless charging," *IEEE Trans. Power Electron.*, vol. 32, no. 8, pp. 5943–5952, Aug. 2017, doi: 10.1109/TPEL.2016.2616111.

[89] A. M. Ahmed and O. O. Khalifa, "Wireless power transfer for electric vehicle charging," in *Proc. 7TH Int. Conf. Electron. DEVICES, Syst. Appl. (ICEDSA)*, 2020, vol. 2306, no. 1, pp. 4–17, doi: 10.1063/5.0032383.

[90] J. Gao, "Traveling magnetic field for homogeneous wireless power transmission," *IEEE Trans. Power Del.*, vol. 22, no. 1, pp. 507–514, Jan. 2007, doi: 10.1109/TPWRD.2006.876645.

[91] Y. Jang, S. Jeong, and M. Lee, "Initial energy logistics cost analysis for stationary, quasi-dynamic, and dynamic wireless charging public transportation systems," *Energies*, vol. 9, no. 7, p. 483, Jun. 2016, doi: 10.3390/en9070483.

[92] A. A. S. Mohamed, C. R. Lashway, and O. Mohammed, "Modeling and feasibility analysis of quasi-dynamic WPT system for EV applications," *IEEE Trans. Transport. Electrific.*, vol. 3, no. 2, pp. 343–353, Jun. 2017, doi: 10.1109/TTE.2017.2682111.

[93] N. Mohamed, F. Aymen, M. Ben Hamed, and S. Lassaad, "Analysis of battery-EV state of charge for a dynamic wireless charging system," *Energy Storage*, vol. 2, no. 2, Apr. 2020, doi: 10.1002/est2.117.

[94] S. Debnath, A. Foote, O. C. Onar, and M. Chinthavali, "Grid impact studies from dynamic wireless charging in smart automated highways," in *Proc. IEEE Transp. Electrific. Conf. Expo (ITEC)*, Jun. 2018, pp. 650–655, doi: 10.1109/ITEC.2018.8450149.

[95] F. Mwasilu, J. J. Justo, E.-K. Kim, T. D. Do, and J.-W. Jung, "Electric vehicles and smart grid interaction: A review on vehicle to grid and renewable energy sources integration," *Renew. Sustain. Energy Rev.*, vol. 34, pp. 501–516, Jun. 2014, doi: 10.1016/j.rser.2014.03.031.

[96] P. Vithayasrichareon, G. Mills, and I. F. MacGill, "Impact of electric vehicles and solar PV on future generation portfolio investment," *IEEE Trans. Sustain. Energy*, vol. 6, no. 3, pp. 899–908, Jul. 2015, doi: 10.1109/TSTE.2015.2418338.

[97] N. Mohamed, F. Aymen, and M. Ben Hamed, "Characteristic of photovoltaic generator for the electric vehicle," *Int. J. Sci. Technol. Res.*, vol. 8, no. 10, pp. 871–876, 2019.

[98] W. Jiang, S. Xu, N. Li, Z. Lin, and B. W. Williams, "Wireless power charger for light electric vehicles," in *Proc. IEEE 11th Int. Conf. Power Electron. Drive Syst.*, Jun. 2015, pp. 562–566, doi: 10.1109/PEDS.2015.7203533.

[99] G. R. Mouli, P. Vanduijsen, T. Velzeboer, G. Nair, Y. Zhao, A. Jamodkar, O. Isabella, S. Silvester, P. Bauer, and M. Zeman, "Solar powered e-bike charging station with AC, DC and contactless charging," in *Proc. 20th Eur. Conf. Power Electron. Appl. (EPE ECCE)*, 2018, p. p-1.

[100] G. A. Shcheglov and L. L. Morozov, "Orbital HPC-center based on solar power satellite," in *Proc. AIP Conf.*, vol. 2318, Feb. 2021, Art. no. 020022, doi: 10.1063/5.0035819.

[101] M. F. Mahmood, S. K. Gharghan, S. L. Mohammed, A. Al-Naji, and J. Chahl, "Design of powering wireless medical sensor based on spiral-spider coils," *Designs*, vol. 5, no. 4, p. 59, Sep. 2021, doi: 10.3390/designs5040059.

[102] A. Hakemi, D. Jovanovic, D. M. Vilathgamuwa, G. Walker, and J. Pauls, "Generic uncertainty parameter analysis and optimization of series–series wireless power transfer system for robust controller design," *IEEE Trans. Ind. Electron.*, vol. 69, no. 4, pp. 4107–4118, Apr. 2022, doi: 10.1109/TIE.2021.3071689.

[103] T. Wang, Q. Xu, W. Jia, Z.-H. Mao, H. Tang, and M. Sun, "Dual-functional wireless power transfer and data communication design for micromedical implants," *IEEE J. Emerg. Sel. Topics Power Electron.*, vol. 9, no. 5, pp. 6259–6271, Oct. 2021, doi: 10.1109/JESTPE.2021.3049787.

[104] S. D. Barman, A. W. Reza, N. Kumar, M. E. Karim, and A. B. Munir, "Wireless powering by magnetic resonant coupling: Recent trends in wireless power transfer system and its applications," *Renew. Sustain. Energy Rev.*, vol. 51, pp. 1525–1552, Nov. 2015, doi: 10.1016/j.rser.2015.07.031.

NAOUI MOHAMED was born in Nefta, Tunis, in 1991. He received the degree in electrical engineering from the University of Gabès, Tunisia, in 2015, and the Ph.D. degree from the Department of Electrical Engineering, in 2020. From 2016 to 2018, he worked as a Professional Engineer in electrical and automatic engineering. He is currently an Associate Professor in electrical engineering with the University of Gabès (ENIG). He has academic experience of three years. He has published over 30 research articles in reputed journals, international conferences, and book chapters. His research interests include electric vehicles, power systems, and renewable energy.

FLAH AYMEN was born in GabeÌs, Tunisia, in 1983. He received the bachelor's and M.Tech. degrees in electrical engineering from ENIG, Tunisia, in 2007 and 2009, respectively, and the Ph.D. degree from the Department of Electrical Engineering, in 2012. He has an academic experience of 11 years. He has published over 40 research articles in reputed journals, international conferences, and book chapters.

TURKI E. A. ALHARBI received the B.Sc. degree (Hons.) in electrical engineering from Umm Al-Qura University (UQU), Makkah, Saudi Arabia, in 2012, the M.Sc. degree (Hons.) in broadband and mobile communication networks from the University of Kent, Canterbury, U.K., in 2016, and the Ph.D. degree in electrical and electronic engineering from the University of Manchester, Manchester, U.K., in 2021. He is currently an Assistant Professor of wireless communication networks with the College of Engineering, Taif University. His current research interests include future key technologies for wireless networks, beyond 5G/6G networks, antenna design, cooperative and energy harvesting networks, NOMA, full-duplex, D2D communication, and SWIPT. He has received many awards and prizes, including the IEEE UKRI Communications Chapter Prize for being Top Distinction Student of the M.Sc. degree. He also received the Rohde and Schwarz Project Prize from the University of Kent for the Best Graduation Project in the telecommunications field.

CLAUDE ZIAD EL-BAYEH received the master's degree in electrical and electronic engineering from the Lebanese University Faculty of Engineering II, Lebanon, in 2008, the M.Sc. degree in organizational management from the University of Quebec, Chicoutimi, Canada, in 2012, the Master of Research degree in renewable energy from Saint Joseph University, Beirut, Lebanon, in 2014, and the Ph.D. degree in electrical engineering and renewable energy from the University of Quebec–École de Technologie Supérieure, Montreal, Canada, in 2019. From 2008 to 2014, he worked as a Professional Engineer in the field of electrical installation in buildings. Since 2015, he has been working in the fields of optimization and energy management for smart buildings, smart grid, electric vehicles, and renewable energy systems.

SBITA LASSAAD was born in Hammam Lif, Tunisia, in 1962. He received the B.E. degree in electrical engineering from the University of Tunis, Tunis, Tunisia, in 1985, and the D.E.A. and Thesis degrees in electrical engineering from the École nationale supérieure d'ingénieurs de Tunis, Tunis, in 1987 and 1997, respectively. In 1988, he joined the Department of Electrical Engineering, National School of Engineering of Sfax, University of Sfax, as a Professor Assistant, and the Department of Electrical Engineering, National Engineering School of Gabes, University of Gabés, Gabés, Tunisia, in 1991, where he became an Associate Professor, in 1998, and a Professor, in 2009.

SHERIF S. M. GHONEIM (Senior Member, IEEE) received the B.Sc. and M.Sc. degrees from the Faculty of Engineering at Shoubra, Zagazig University, Egypt, in 1994 and 2000, respectively, and the Ph.D. degree in electrical power and machines from the Faculty of Engineering, Cairo University, in 2008. Since 1996, he has been teaching with the Faculty of Industrial Education, Suez Canal University, Egypt. From 2005 to 2007, he was a Guest Researcher with the Institute of Energy Transport and Storage (ETS), University of Duisburg–Essen, Germany. He joined the Electrical Engineering Department, Faculty of Engineering, Taif University, as an Associate Professor. His research interests include grounding systems, dissolved gas analysis, and breakdown in SF6 gas.

URSULA EICKER is currently the Canada Excellence Research Chair (CERC) for next generation cities at Concordia University Montréal. A German physicist, she has held leadership positions at the Stuttgart University of Applied Sciences and its Centre for Sustainable Energy Technologies. Since June 2019, she has been leading an ambitious research program to establish transformation strategies toward zero-carbon cities. Her main research interests include urban scale modeling, zero carbon buildings, renewable energies, and circular economy strategies.